

**Instituto Tecnológico y de Estudios Superiores
de Monterrey
Campus Monterrey**



**Analysis of Resource Allocation in Wireless Mobile
Systems with Orthogonal Frequency Division Multiplexing**

by

Ing. Yaztmin Cruz Guerrero

Thesis

**Presented to the Program of Graduate Studies in
Information Technologies and Electronics In partial
fulfillment of the requirements for the degree of**

**Master of Science
in Electronic Engineering
Major in Telecommunications**

May, 2011.

**Instituto Tecnológico y de Estudios Superiores
de Monterrey**

Campus Monterrey



**Analysis of Resource Allocation in Wireless Mobile
Systems with Orthogonal Frequency Division Multiplexing**

by

Ing. Yazirmin Cruz Guerrero

Thesis

**Presented to the Program of Graduate Studies in
Information Technologies and Electronics In partial
fulfillment of the requirements for the degree of**

Master of Science

in Electronic Engineering

Major in Telecommunications

May, 2011

Instituto Tecnológico y de Estudios Superiores de Monterrey

Campus Monterrey



**Analysis of Resource Allocation in Wireless Mobile Systems with
Orthogonal Frequency Division Multiplexing**

by

Ing. Yaztmin Cruz Guerrero

Thesis

Presented to the Program of Graduate Studies in Information Technologies and Electronics

In partial fulfillment of the requirements for the degree of

Master of Science

in Electronic Engineering

Major in Telecommunications

May, 2011

© Yaztmin Cruz Guerrero, 2011

God, thanks for give me the intelligence, wisdom and strenght to do everything, for bless me everyday, for take care of me and because you had been with me at all the times. Thanks God because without you I would never have achieved it. You are the best.

I dedicate this work with love
To my parents Felipe and Raquel,
To my sisters and brothers, Marlén, Elia, René and Lino
To who makes me smile always, Issac

But he said to me, "My grace is sufficient for you, for my power is made perfect in weakness."

2 Corinthians 12:9

Reconocimientos

To my parents for every word of encouragement, your patience and understanding.

I am grateful to my thesis advisor César Vargas Rosales because he was always very patient with me and it showed some of their knowledge and time on me. Besides, I wish to give my complete appreciation to my synods, Dr. Jose Ramon Rodriguez and Ing. Artemio Aguilar for their comments and suggestions to improve this thesis.

To my brother and sister Marlen, Elia, Rene and Lino, because although I was away they always were with me. To all my nephews because they showed me their love.

Especially to Isaac because he was always with me, for every word of faith, prayers, patience and love.

To my friends Gaby, Lisa, Bere, Denisse and Paty, for your prayers and for their sincere friendship.

To all my classmates because they always helped me and for their friendship Fernando, Ivan, Alberto, Cesar, Raul, Tania, Fernando, Hector.

To my cousin Pepe and his family because they made me feel at home.

YAZTMIN CRUZ GUERRERO

Instituto Tecnológico y de Estudios Superiores de Monterrey

Mayo 2011

Analysis of Resource Allocation in Wireless Mobile Systems with Orthogonal Frequency Division Multiplexing

Yaztmin Cruz Guerrero, M. Sc.

Instituto Tecnológico y de Estudios Superiores de Monterrey, 2011

Thesis Advisor: César Vargas Rosales, Ph. D.

Nowadays, there are wireless systems that offer different class of services with large bandwidth requirements. Nevertheless, to share their resources, such systems have to develop models in order to allocate those resources among costumers.

Moreover, this kind of systems has to counteract the effects of lossy channel, so Orthogonal Frequency Division Multiplexing (OFDM) is implemented by them. Researches have been done related to allocate the resources, being the Quality of Service (QoS) the main goal.

This thesis is focused on the carrier, in other words, a mathematical model is derived taking into account the mobility of users and the system capacity instead of the QoS. Thus, the model has long been modified to show the influence of the channel conditions.

Both models are developed as an s -dimensional birth- death process. The mobility of a user in the system is modeled by different probabilities in the case of the session termination and of the handoffs.

To show the performance of the system, the blocking probability and the net revenue are presented. Finally numerical results are showed for different levels of mobility of the model derived.

Contents

Reconocimientos	v
Abstract	vii
List of Tables	xi
List of Figures	xiii
Chapter 1 Introduction	1
1.1 Previous Work	2
1.2 Problem Statement	3
1.3 Objectives	3
1.4 Justification	3
1.5 Organization	4
Chapter 2 Multicarrier transmission	5
2.1 Introduction	5
2.2 Multicarrier transmission	6
2.2.1 Basic principles of OFDM	9
2.2.2 OFDM-based Wireless Communication Systems	13
Chapter 3 Model Description	19
3.1 Model for resource allocation	19
3.2 Model for channel-aware resource allocation.	25
3.2.1 Net Revenue	29
Chapter 4 Numerical Results	31
4.1 Resource allocation in OFDM systems regardless channel conditions	32
4.1.1 Blocking results	33
4.1.2 Net revenue results	38

4.2	Model for channel-aware conditions resource allocation.	40
4.2.1	Blocking results	41
4.2.2	Net revenue results	44
Chapter 5 Conclusions		47
5.1	General Conclusions	47
5.2	Future work	48
Bibliography		49
Vita		53

List of Tables

2.1	Channel bandwidth divided into resource blocks in LTE	15
4.1	Simulation parameters	33
4.2	Parameters for mobility for the three cells.	33
4.3	Parameters for mobility with $q_{1cc1}^{(s)} = 0$ and $q_{1ee1}^{(s)} = 0$	38
4.4	Parameters for net revenue.	39

List of Figures

2.1	Multipath propagation, [10].	5
2.2	Interference intersymbol of a high data rate stream.	6
2.3	Serial to parallel transmission with $k = 8$ subcarriers using a total bandwidth of BW	8
2.4	Multicarrier transmission scheme.	9
2.5	Spectrum of N orthogonal subcarriers separated by Δ_f	9
2.6	Increasing the modulation symbol duration by N times.	10
2.7	Digital implementation for transceiver OFDM, [11].	11
2.8	Transceiver OFDM with Cyclic Prefix added, [11].	12
2.9	Subsets of adjacent subcarriers for downlink and uplink, [10].	13
2.10	Subsets of distributed subcarriers for downlink and uplink, [10].	13
2.11	Orthogonal subcarriers: the desired subcarrier has maximum value while other ones have zero value, [20].	14
2.12	Example of the division of the $BW_E = 9$ MHz in subcarriers which in turn are grouped into resource blocks.	15
2.13	Difference between the transmission of an OFDM symbol and an SC-FDMA symbol, [23].	16
2.14	Subcarrier allocation for three users with 12 subcarriers each one.	17
2.15	Division of a OFDM channel in WiFi5, [27].	18
3.1	Circle area proportion	20
3.2	Seven-cell hexagonal system with soft frequency reuse scheme	20
3.3	Resource blocks as capacity for center and edge area of each cell.	21
3.4	Three-cell hexagonal system with interaction between them.	22
3.5	Birth-death process of a cell with $s=2$, $C=6$, $b_1 = 1$ and $b_2 = 3$	23
3.6	2-dimensional birth-death process with $C=6$, $b_1 = 1$ and $b_2 = 3$	24
3.7	Description of the evolution of a lossy channel in a wireless network.	26
3.8	2-state Markov chain that describes a digital communication channel.	26
3.9	2-dimensional birth-death process with $RB_1 = 6$, $RB_2 = 3$, $n_1 = 1$ and $n_2 = 2$	28

4.1	3-cell hexagonal network.	32
4.2	Capacity for eah area at cell l	33
4.3	Blocking probability where is no mobility for center area of cell 1.	34
4.4	Blocking probability without mobility for edge area of cell 1.	34
4.5	Network blocking probability without mobility, $q_{lT}^{(s)} = 1$	35
4.6	Blocking probability for each service at center of cell 1, with low mobility.	36
4.7	Blocking probability with low mobility for edge area of cell 1.	36
4.8	Blocking probability with low and high mobility for cell 1.	37
4.9	Blocking probability of cell 2 where low and high mobility is considered.	37
4.10	Network blocking probability with low and high mobility.	38
4.11	Comparison of blocking probability for cell 1, $q_{1cc1}^{(s)} \neq 0$, $q_{1ee1}^{(s)} \neq 0$ and $q_{1cc1}^{(s)} = q_{1ee1}^{(s)} = 0$. 39	
4.12	Comparison of blocking probability for the network, $q_{1cc1}^{(s)} \neq 0$, $q_{1ee1}^{(s)} \neq 0$ and $q_{1cc1}^{(s)} = q_{1ee1}^{(s)} = 0$	39
4.13	Comparison of the net revenue generated with different levels of mobility.	40
4.14	Net revenue wit different levels of mobility.	40
4.15	Bloking probability when a subcarrier go from a bad state to good state with different rates.	41
4.16	Bloking probability for all services at cell-center 1.	42
4.17	Comparison of network blocking for no mobility, under reliable and unreliable channel. 43	
4.18	Comparison of blocking for the network with and without mobility.	43
4.19	Network blocking when a resource block has 1 and 2 subcarriers under bad channel conditions.	44
4.20	Comparison of the net revenue generated with a reliable and unreliable channel. . . 45	
4.21	Net revenue with low mobility with and without channel conditions.	45
4.22	Net revenue with 1 and 2 subcarriers under bad channel conditions.	46

Chapter 1

Introduction

In these days mobile communication systems have to give higher capacity, bit rate and bandwidth to users, because they use applications such as mobile TV, online gaming, multimedia streaming , etc. Moreover, sophisticated devices are emerging and people want to be walking or driving while they are connected each other.

The number of users in wireless mobile systems is growing, while the bandwidth that a system has is the same. This kind of systems has to face the issue that the bandwidth is a scarce resource, so it is needed to improve its use. So that more users can be served, because if a user requests a service to a wireless network he must find an available channel. Another important aspect that must be taken into account is to counteract the bad effects produced by the channel like intersymbol interference (ISI) and the situations when the conditions are so bad that the session of a user can not be established.

Most of the times the carrier is the one who offers the services in wireless systems, these services can have different bandwidth requirements, so the best way to meet the requests of service of the mobile users must be found. A performance measure that shows to the carrier the behavior of its network is the blocking probability. Other effect that has to be evaluated is the handoff, i.e., when an active user moves from one cell area to other area of the same cell or to other cell. This effect can be seen in the net revenue, which is very important for the carrier because it gives it information about its profits.

So this work wants to develop a model that shows to a carrier how to allocate resources to users according to the class of service, taking into account the channel conditions and the capacity of the system. After, we consider different levels of mobility to see their effects on the blocking probability and on the net revenue.

This model is derived as a multi-dimensional Markov chain, because the system provides more than one class of service [1]. To diminish the intersymbol interference caused by the channel we use Orthogonal Frequency Division Multiplexing (OFDM) where the total bandwidth is split into narrower subchannels termed subcarriers, which will be grouped in blocks (resource blocks) and

then allocated to a user. Moreover, we use the channel model given by Gilbert-Elliot to describe the behavior of the wireless channel.

1.1 Previous Work

Since the world of telecommunications has progressed very fast, some researches have been done to exploit the spectrum for a wireless system and some algorithms for resource allocation considering OFDM as the multiplexing scheme has been derived.

A system can have multiple classes of customers with different bandwidth requirements as well as with different statistical characteristics for arrival rate and service, so can not be lumped into a single class for its analysis. These kind of systems with K costumers types are analized with chains termed multi-dimensional Marcov chains, [1]. We use this kind of model in order to explain the evolve of the cell occupancy, because the wireless system to be analized has many services. Others researches that use this kind of chains is [2], where m classes of traffic are sharing the total capacity of a network and the other one is [3]. Although this works is focus in developing a call admision protocol we see that a system with s classes of services can be modeled with a multi-dimensional Markov chain.

The first work does not use OFDM, and does not take into account the lossy channel in order to allocate the resources. The former is used in our work because the channel presents some effects on the signal that affects its reception. For example, if the bandwidth of the transmitted signal is higher than that of the coherence bandwidth of the channel (where the channel conditions are highly correlated), the signal will be corrupted. With the use of OFDM we increase the robustness against this channel effects.

About the allocation of the subcarrier in an OFDM system researches have been developed one of them is presented by [4] where the allocation is focused on the maximization of the throughput of the users, i.e., it searches the users that have the best channel conditions in order to assign him subcarriers. Other research has been done by [5] where it is explained that the allocation of subcarriers is done according to the QoS required by the users. This work considered a service's cost too, but their results are expressed in terms of total power consumption, so they focus on the QoS. In [6] the assignment of subcarriers is done according the QoS that is translated in the minimum guaranteed rate. The total revenue of the network is studied too, which is maximized when the throughput of the users is high. In [2] the net revenue is calculated, but in this case for different levels of mobility.

1.2 Problem Statement

The wireless communications are seriously affected by two situations. The former issue is because the spectral resource is limited and the latter because the transmission medium is the radio channel.

So the providers of wireless mobile services termed as carriers have to make efficient all their bandwidth. Thus, more users can be provided with service. The other issue that has to counteract is to minimize the effects of the channel on the signal transmission.

The subcarrier allocation in, [7], is done under the constraint of the transmit power and the Bit Error Rate (BER), while their goal is to maximize the total data rate of the users. Other algorithm to allocate resources is given by [8], who wants to find the best allocation option that requires a lowest total transmit power while the BER as Quality of Service (QoS) is met. The results shown by the former are the average data rate according to the number of users or subcarriers and for the latter is the total transmit power given a number of users in the system.

This is very important for the users, but we want to focus on the carrier. Thus this work must derive a model that analyzes the resource allocation in the wireless system, as well as the handoffs of the costumers. Therefore, some performance measures like the blocking probability, must be obtained to help the carriers get information about the behavior of its network. Because, their profits depend on them, mainly the net revenue has to be maximized.

1.3 Objectives

This work wants to analyze the performance of a mobile system with a model developed to share resources.

Specific objectives are listed below

- To obtain a mathematical model showing the behavior of a wireless network under different levels of mobility, which takes into account only the resources available. On the other hand it modifies the model to include the channel's effects on the assignment.
- To derive a model of the net revenue for the system to see the difference when channel effects are taken into account, as well as the mobility.

1.4 Justification

Currently the quantity of users that are served by a wireless mobile network is growing, so that the bandwidth of a system has to be shared. Some researches has been developed to allocate

to users resources taking into account the channel behavior, they do it to maximize the QoS, since the requirements to do it is when some parameters like bit error rate, signal to noise ratio have to meet an requirement. Moreover sometimes the algorithm of these researches is complex because many comparisons must be made in order to allocate resources to a user, which implies higher computational complexity.

Then we have to develop a model that exploit the bandwidth as first requirement, then allocate the resources considering the channel conditions and finally giving performance measures under mobility conditions. All this so that the carriers evaluate its network's performance.

1.5 Organization

This work is composed of five chapters. Chapter 1 presents an introduction to this work as well as the objectives and the motivation to do it. Chapter 2 presents the background of OFDM used as a technique of multicarrier transmission, where concepts as subcarrier, resource blocks and multicarrier transmission are defined to understand why OFDM is widely used, and also we present wireless communications systems that currently are using it. Chapter 3 shows the derivation of the model to describe how the capacity is shared in a system with and without channel conditions, its structure and the mathematical model to calculate the net revenue. Chapter 4 is focus in the numerical results where the discussions of them are given. And finally Chapter 5 includes the conclusions of this work.

Chapter 2

Multicarrier transmission

In this chapter we explain what the multicarrier transmission is, the characteristics of Orthogonal Frequency Division Multiplexing (OFDM) which is one of the transmission techniques used in wireless communications, as well as some of the technologies that are currently using OFDM, for example Long Term Evolution (LTE) and WiFi5 (811.2a).

2.1 Introduction

One of the goals of mobile communications is to provide higher transmission rates, so that wider bandwidths are necessary. In order to achieve that goal, the system needs to cope with corrupted signals to be received. Delay spread and frequency selective fading arise, the former because the signal transmitted arrives via multiple paths, as shown in Figure 2.1, as a superposition of signals with different amplitudes, phases and delays, causing data pulses to overlap, producing *intersymbol interference* (ISI) as shown in Figure 2.2. The latter is because the channel frequency response is not constant, so the signal will be corrupted, [9], [10].

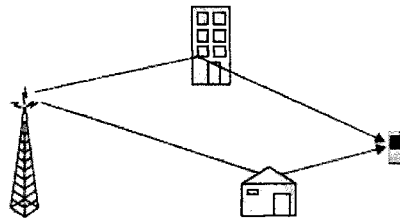


Figure 2.1: Multipath propagation, [10].

One way to counteract this phenomena maintaining at the same time high data rates and wider bandwidths is to use multi-carrier transmission. *Multi-carrier transmission*, is used to transmit several narrower bandwidth signals (hence forth called *subcarriers or tones*), which are multiplexed to transmit them to the receiver via the same radio link, instead of transmitting a single wider bandwidth signal, [11], [10].

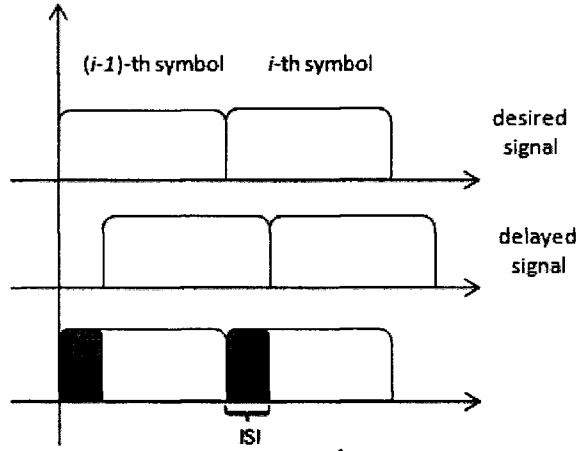


Figure 2.2: Interference intersymbol of a high data rate stream.

2.2 Multicarrier transmission

Propagation in the radio environment is affected by the multipath propagation. So, the mobile radio channel is characterized in the time domain by the time variance and in the frequency domain by the frequency selectivity.

The time domain is characterized by the speed difference between the receiver and the transmitter v , and by the wavelength λ , the relation between them is done by the so called Doppler frequency shift given by

$$\nu = \frac{v}{\lambda} \cos(\theta) = \frac{v}{c} f_0 \cos(\theta) = \nu_{max} \cos(\theta), \quad (2.1)$$

where

c : velocity of the light

f_0 : transmit frequency

θ : angle between the direction of the received signal and the direction of motion

as we can see $\nu = \nu_{max}$ when $|\cos\theta| = 1$, i.e. $\theta = 0, \pi$.

Now, if we transmit a signal at f_0 , because of the multipath the signal arrives with different phases producing constructive or destructive interference, so the received signal in the time domain will be varying in amplitude too, the last is called *fading*. Then we can say that the signal is modulated in amplitude and phase by the channel.

When the modulation of the carrier is done by a digital phase, for example M -PSK, it may have problems if the phase of the signal changes a lot during T_s (time to transmit a symbol modulated digitally). If we relate the variation in the frequency with the variation in time, will have a time scale as

$$t_{corr} = \frac{1}{v_{max}}, \quad (2.2)$$

where t_{corr} is called correlation time (time duration where channel variations have high correlation). If $t_{corr} < T_s$ we will have a *time selective channel*, therefore the signal will be under high phase changes. So to have a good digital transmission we requires $T_s \ll t_{corr}$, i.e.

$$T_s \ll \frac{1}{v_{max}}, \quad (2.3)$$

$$v_{max}T_s \ll 1. \quad (2.4)$$

The other characterization, is the frequency selectivity. The bandwidth of the channel that has channel variations with high correlation, is called *coherence bandwidth* or *correlation frequency*. Now, if the bandwidth of the signal is higher than that bandwidth we will have a frequency selective channel, [12]. The correlation frequency is given by

$$f_{corr} = \frac{1}{\tau}, \quad (2.5)$$

where τ is the *delay spread* (time difference between the arrival of the first and the last component multipath), [13].

Now, assume a digital transmission scheme with M -PSK as carrier modulation, where the symbol duration is T_s and the bandwidth given by $BW = 1/T_s$. If we want to receive data without ISI, the delay spread (τ) has to be less than symbol duration time T_s , i.e., there will be *frequency-nonselective* so the bandwidth of the signal will be less than the frequency of correlation given by $BW \ll f_{corr}$, that is

$$BW \ll \frac{1}{\tau}, \quad (2.6)$$

$$BW\tau \ll 1, \quad (2.7)$$

$$\tau \ll T_s. \quad (2.8)$$

$$(2.9)$$

Consider a system with only a single carrier, then the bit rate is $R_b = \log_2(M)T_s^{-1}$ where we observe that the R_b is limited by the delay spread of the channel, [14]. To overcome this limitation the multi-carrier transmission is used, it means that a serial data stream with high rate are split into k parallel, [15], substreams with low rate, and each of them modules a different subcarrier,

see Figure 2.3 for $k = 8$. In this case in the frequency domain is seen as a parallel transmission, where the overall bandwidth is the same if the transmission were only using a single carrier. With this division the T_s is incremented k times, and the bandwidth of each subcarrier is B/k , [14].

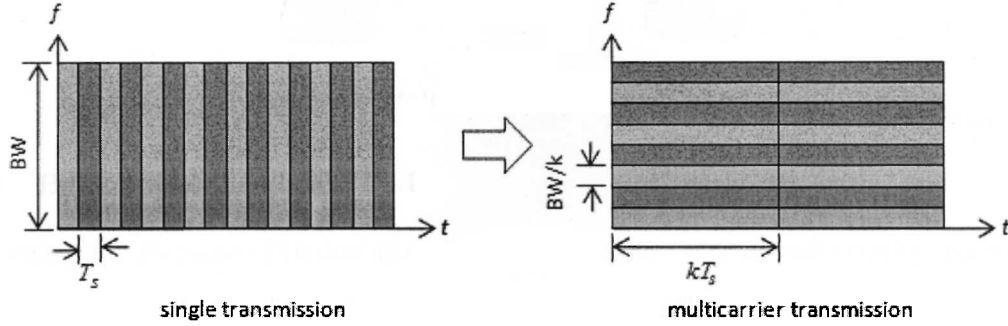


Figure 2.3: Serial to parallel transmission with $k = 8$ subcarriers using a total bandwidth of BW .

But, k has a limit, because the symbol duration time has to be less than time correlation so equation 2.4 has to be fulfilled, otherwise the symbol will be under a *time selective channel* and therefore the symbol will be corrupted. In order to meet simultaneously the requirement established by this equation and the equation 2.9 the coherency factor $\kappa = \nu_{max}\tau$ has to accomplish the requirement $\kappa \ll 1$.

There are two ways to implement multicarrier transmission, in the first one k subcarriers will be modulated individually, while in the second one, parallel data substreams excites an array of k adjacent bandpass filters, [14]. We will focus on the second option, because OFDM uses a bank of filters that can be implemented using the Fast Fourier Transform.

In the second option a basis pulse $g(t)$ is used, which has frequency-shifted replicas as $g_k(t) = e^{j2\pi f_k t} g(t)$, for example, if $g(t) = g_1(t)$, then $f = 1$ and each $g_k(t)$ will have $f = f_k$. The k (or $k+1$) symbols to be transmitted will use different pulse shapes $g_k(t)$ in each time instant l , it means that each sub stream will pass trough a different bandpass filter, see Figure 2.4. The outputs are added and then are transmitted by a same RF. The complex baseband signal to be transmitted is, [14],

$$s(t) = \sum_l \sum_k s_{kl} g_k(t - lT_s), \quad (2.10)$$

where $g_k(t)$ is the pulse shape in the time instant l and frequency k , given by

$$g_k(t - lT_s) = e^{j2\pi f_k(t - lT_s)} g(t - lT_s). \quad (2.11)$$

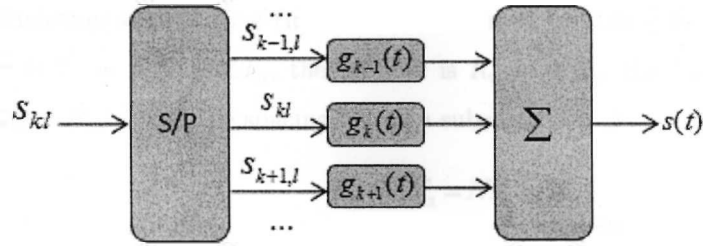


Figure 2.4: Multicarrier transmission scheme.

2.2.1 Basic principles of OFDM

Orthogonal Frequency Division Multiplexing (OFDM) is a kind of multi-carrier transmission that exploits bandwidth because of orthogonal subcarriers, where the subcarrier spacing is lower than that of Frequency Division Multiplexing (FDM). OFDM splits the information in blocks of N symbols; it means that a serial data stream with high data rate is divided into data streams of N parallel symbols which have a lower data rate. Those symbols will be transmitted by modulating N lower bandwidth subcarriers. In the time domain each subcarrier modulated has rectangular shape, so its spectrum has a $\sin(x)/x$ shape, as can be seen in Figure 2.5, [11].

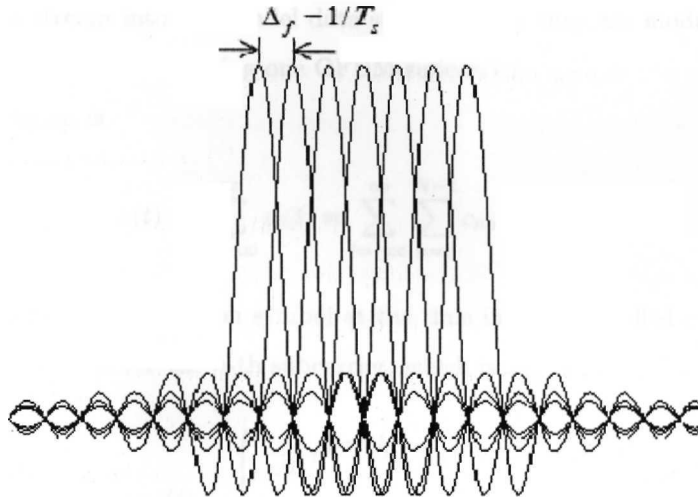


Figure 2.5: Spectrum of N orthogonal subcarriers separated by Δ_f .

As an example consider a data stream that is divided in blocks of five modulation symbols, so the bandwidth BW will consist of five subcarriers to be modulated by them, then the outputs are added to produce an OFDM symbol. After conversion of the data stream from series to parallel, the modulation symbol will be N times larger, so each symbol OFDM will have the same duration, then the harmful by multipath echoes will be lower. It can be seen the Figure

2.6, where the modulation symbol time (in this case is formed by only a bit) is T_u , so the time on each subcarrier is $T_s = NT_u = 5T_u$, the bit rate is $R_u = NR_s$, the Baud rate is given by $R_s = 1/T_s = 1/NT_u = R_u/m$ and the spacing between subcarriers is $\Delta_f = 1/T_s$.

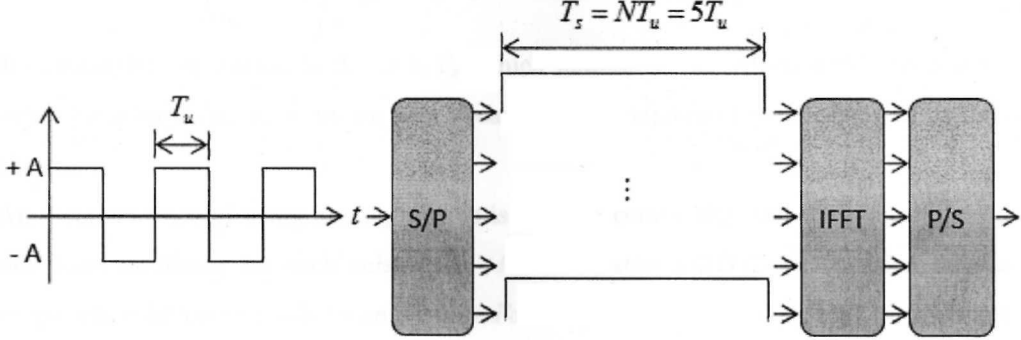


Figure 2.6: Increasing the modulation symbol duration by N times.

Implementation

An analog scheme for OFDM transmission has a data source followed by a block S/P in order to split serial data stream into N parallel data streams, then they are modulated by N complex modulators, each of them representing one OFDM subcarrier.

The OFDM signal is

$$s(t) = \sum_{i=-\infty}^{\infty} s_i(t) = \sum_{i=-\infty}^{\infty} \sum_{n=0}^{N-1} c_{n,i} g_n(t - iT_s), \quad (2.12)$$

where $c_{n,i}$ is the complex modulation symbol at the time instant i applied on the n -th subcarrier and $g_n(t)$ is the wave form for the n -th subcarrier, which is

$$g_n(t) = \begin{cases} \frac{1}{\sqrt{T_s}} e^{j2\pi n \frac{t}{T_s}} & \text{for } 0 < t < T_s \\ 0 & \text{otherwise.} \end{cases}$$

If only the i -th OFDM symbol is considered, this is expressed in the interval $iT_s \leq t \leq (i+1)T_s$ as

$$s_i(t) = \frac{1}{\sqrt{T_s}} \sum_{n=0}^{N-1} c_{n,i} e^{j2\pi n \frac{t}{T_s}}, \quad (2.13)$$

where the modulation symbol can be obtained from different modulation schemes, such as QPSK, 16QAM or 64QAM.

Now, if we take two modulated subcarriers in $iT_s \leq t \leq (i+1)T_s$ the orthogonality between them is because the following relation is fulfilled

$$\int_{iT_s}^{(i+1)T_s} c_{n1}c_{n2}^* e^{j2\pi n_1 \frac{t}{T_s}} e^{j2\pi n_2 \frac{t}{T_s}} dt = 0 \quad \text{for } n_1 \neq n_2, \quad (2.14)$$

and the subcarrier separation is $\Delta_f = 1/T_s$, which maintains the orthogonality with a very low separation between them, this can be seen because the maximum of a subcarrier is in the null of the other ones.

An inconvenience of using analog scheme is its high complexity and cost, since it needs high precision local oscillator for each subcarrier. An alternative OFDM transmission scheme is to subject the modulation symbols to an *Inverse Fast Fourier Transform* (IFFT), to transmit them later. Consider an OFDM symbol, for example for the time $i = 0$, and sample it at instances $t_k = kT_s/N$, to obtain

$$s_k = s(t_k) = \frac{1}{\sqrt{T_s}} \sum_{n=0}^{N-1} c_{n,0} e^{j2\pi n \frac{k}{N}}. \quad (2.15)$$

If we observe, this is the *Inverse Discrete Fourier Transform* (IDFT) of each symbol, therefore we can use a digital transceiver as shown in Figure 2.7, where the IDFT is realized by the IFFT block, and the number of samples (number of symbols) is the same as the number of subcarriers and the size of the samples regularly is a power of 2, and at the output there will be N values to be the input of a P/S block to be transmitted.

The receiver does the reverse operation, i.e., the signal reaching the transmitter passes through an S/P conversion, then the *Fast Fourier Transform* (FFT) is performed to obtain the estimate \tilde{c}_n of c_n , [11], [10].

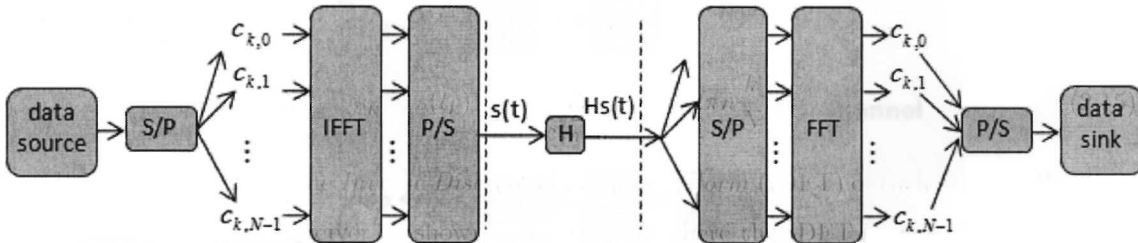


Figure 2.7: Digital implementation for transceiver OFDM, [11].

Cyclic-prefix

Although subcarriers are orthogonal, the time dispersive channel causes not only interference between them and frequency-selective fading, but also intersymbol interference, as a result of a

corrupted signal being received. So a way to reduce this interference is to use a *cyclic prefix* (CP). The received signal is the result of the linear convolution between the signal transmitted and the channel impulse response, so the length of the symbols in the receiver will be higher, this means that the length of the symbol is N and the length of the channel impulse response is L , then the length of the convolution of them is $N + L - 1$. If the following symbol is transmitted immediately afterwards, there will be an overlap of length $L - 1$ on it. This is the reason of the CP, that is to add the last $L - 1$ samples of the transmission symbol at the beginning of it. Now, the duration changes of T_s to $T'_s = T_s + T_{CP}$, [16], [11].

On the receiver side, the first block composed by filters will remove the cyclic prefix, then the remainder will be a cyclic convolution of the transmitted signal and the channel impulse response. The transceiver with CP is shown in Figure 2.8. The data stream is S/P converted. Each block is subjected to IFFT and then the last $L - 1$ samples are prepended. The signal is modulated on a carrier and sent by the radio channel, which adds noise. At the receiver the cyclic prefix is removed from the signal, then passes through an S/P conversion, the remainder is subjected to *Discrete Fourier Transform* implemented by the *Fast Fourier Transform* (FFT), the output is divided by the channel attenuation, i.e. the samples are equalized, to get \tilde{c}_n of c_n , [11].

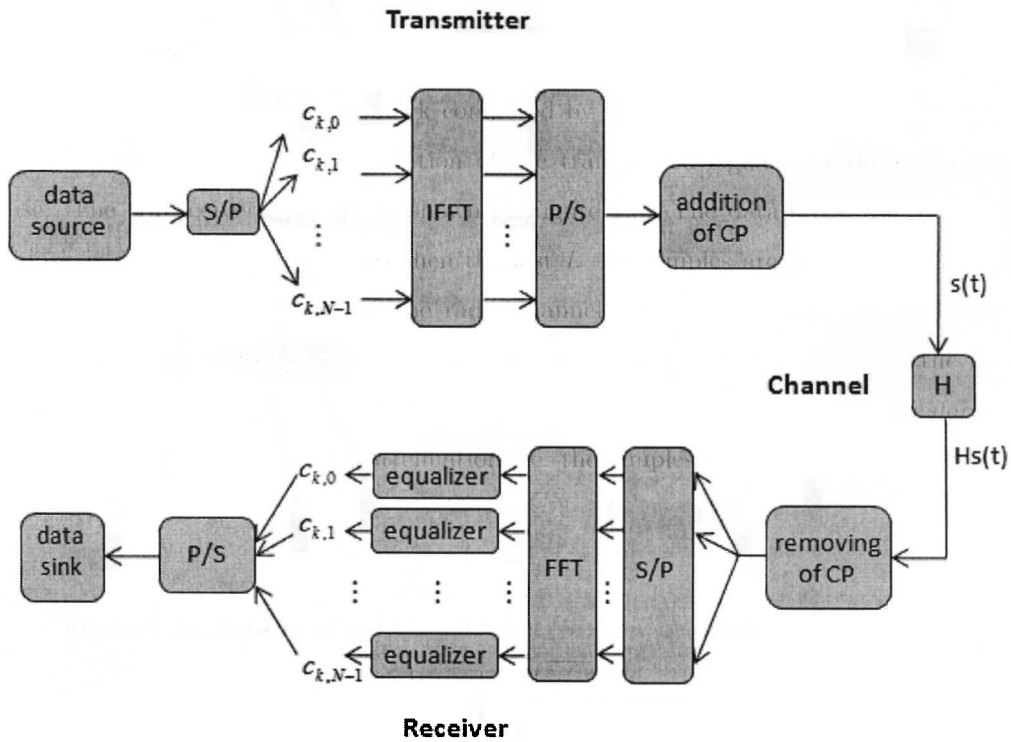


Figure 2.8: Transceiver OFDM with Cyclic Prefix added, [11].

In OFDM systems the condition of the channel of each sub-band needs to be estimated, a method is to use *pilot symbols (reference symbols)*. The information of the estimation is useful in order to use subbands with the best condition (high signal strength), because more bits can be sent using these subcarriers and those with low quality will take fewer bits, so symbols of each subcarrier will be able to use different modulation schemes, [11].

2.2.2 OFDM-based Wireless Communication Systems

Orthogonal frequency division multiplexing not only can be use for s single mobile user, i.e. OFDM can be used as a multiple access scheme, where different subsets of subcarriers are assigned for each mobile user. In the downlink in a OFDM symbol time many users can be served using different subsets of subcarriers, while the uplink data transmission are received from different users using different subsets of subcarriers of all available.

Subcarriers subsets used for transmission to/from user equipment can be grouped in two ways: in adjacent way, subcarriers are contiguous and in interleaved way, subcarriers are equidistant from each, this is illustrated by figures 2.9 and 2.10 respectively, [10]. .

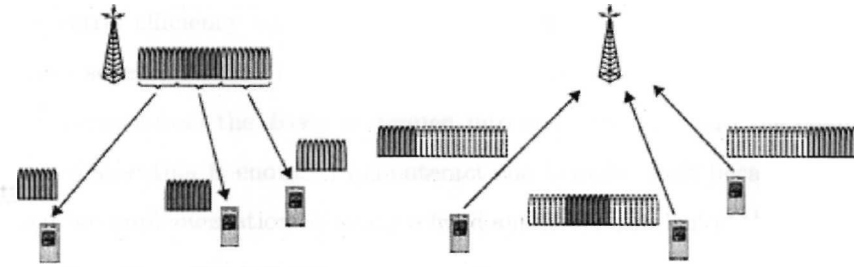


Figure 2.9: Subsets of adjacent subcarriers for downlink and uplink, [10].

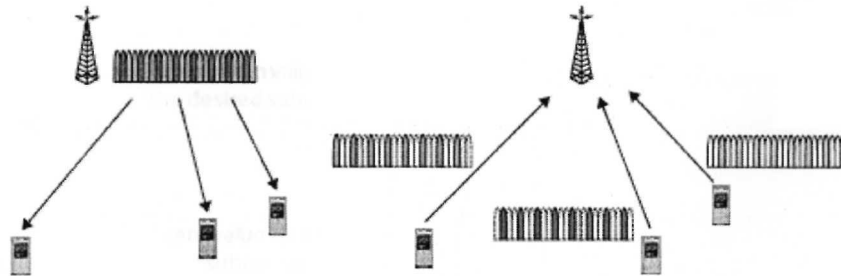


Figure 2.10: Subsets of distributed subcarriers for downlink and uplink, [10].

Because of its robustness against signal corruption, OFDM is being used by some technologies as *multiple-access scheme*, such as *WiFi5 (IEEE.811a)* and *Long Term Evolution (LTE)*. Each of them will be explained in the following.

Long Term Evolution (LTE)

Long Term Evolution is the standard for the fourth-generation (4G) mobile systems created by the *3rd Generation Partnership Project* (3GPP) in response to the requirements of the *International Telecommunication Union* to provide services like mobile TV, online gaming, multimedia streaming, etc. with higher peak data rate, quality and lower latency, [17], [18].

OFDMA in LTE

Long Term Evolution has been designed to provide peak data rates of 300 Mb/s in the DL and 75 Mb/s in the UL with antenna configuration of 4x4 MIMO, a radio-network delay below 5 ms in a bandwidth of 20 MHz, addressing bandwidth scalable for 1.4, 3, 5, 10, 15, 20 MHz, among others, [19].

From now on we will focus on the technique of multiple-access scheme used for the fourth-generation of mobile communications. LTE as stated has different channel bandwidths, BW_i where $i = 1.4, 3, 5, 10, 15, 20$ MHz, but with an effective bandwidth of $BW_E = BW_i - BG$, channel bandwidth less band guard, where $BG = 0.1BW_i$. This standard in order to meet the requirements about higher spectral efficiency with a low cost per bit at the same time, has selected OFDM as a multiple-access scheme for the downlink. Remember that this technique is an example of a multicarrier transmission so the BW_E is divided into subcarriers, where the channel spacing is $\Delta_f = 15$ kHz, because this is enough to counteract the Doppler shift because of the velocity or imperfections in the implementation. The Δ_f is fixed and is independent of the channel bandwidth. As was mentioned in the implementation section, since the subcarriers are orthogonal the adjacent subcarriers have zero value when the desired subcarrier is sampled, as depicted in Figure 2.11, [20].

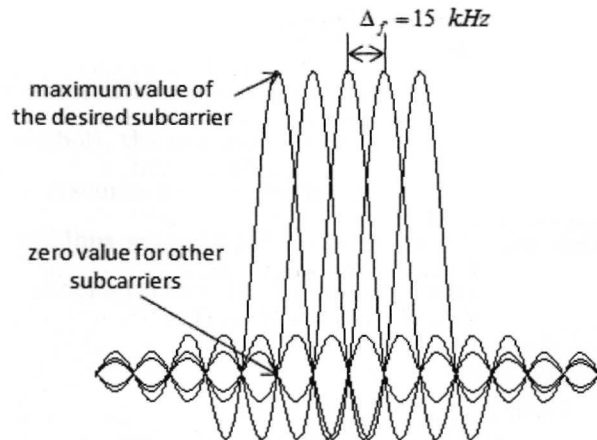


Figure 2.11: Orthogonal subcarriers: the desired subcarrier has maximum value while other ones have zero value, [20].

Since each BW_E is divided by Δ_f , we have different number of subcarriers N_{SC} , which are grouped in the frequency domain into subsets named *resource blocks* with a number of subcarriers n of 12 each, so the minimum bandwidth allocated to a user will be 180 kHz, as it can be seen in Figure 2.12. Therefore in LTE the number of resource blocks ranges from 6 to 100 corresponding to a effective bandwidth ranging from around 1 MHz up to 18 MHz, [10]. The Table 2.1 shows a resume of the transmission bandwidth with its respective split.

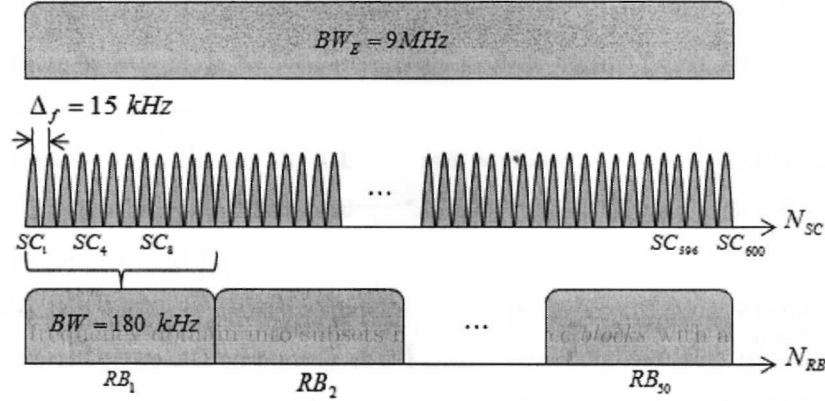


Figure 2.12: Example of the division of the $BW_E = 9\text{ MHz}$ in subcarriers which in turn are grouped into resource blocks.

Table 2.1: Channel bandwidth divided into resource blocks in LTE

Channel bandwidth BW_i (MHz)	1.4	3	5	10	15	20
Effective bandwidth BW_E (MHz)	1.08	2.7	4.5	9	13.5	18
Subcarrier spacing Δ_f (kHz)	15					
Total number of subcarriers N_{sc}	72	180	300	600	900	1200
Number of subcarriers per resource block n	12					
Number of resource blocks N_{RB}	6	15	25	50	75	100

For a system with the higher bandwidth (20MHz) included in the Table 2.1 the raw symbol rate is 18Mbps, where for each 15kHz subcarrier that is 15ksps. If the modulation scheme used is 64QAM (6 bits by symbol), the raw capacity is 108Mbps. Since the minimum resource to be allocated to a user is a resource block (180kHz), the raw symbol for him is 180ksps, whereas the raw capacity is 1.080Mbps when 64QAM is being used for the modulation, [21]. About the spectral efficiency this technology offers 5bits/s/Hz on the downlink and 2.5 bit/s/Hz on the uplink.

SC-FDMA in LTE

Although OFDMA is a good option for the downlink is not for the uplink, as this has a high peak to average power ratio (PAPR). OFDM in the frequency domain is made up of many subcarriers, which in the time domain are several sinusoidal waves added with their respective

frequency and with a channel spacing of 15 kHz, so the envelope of the signal OFDM has very pronounced fluctuations.

If we use this for the uplink we will have a low power efficiency or the output power of the power amplifier of the user equipment may be lower, ie, the amplifier will need to use more back-off if it is fed by a signal with a high envelope variation as is the case of OFDM compared to a single carrier signal.

As a result the uplink range can be lower or the battery energy lasts less because the power amplifier has more consumption although the same average output power level is maintained. For the UL the latter is not a problem because it is the base station, which is large in volume and is connected to the mains but for the UL the user equipment only has its battery. This is the reason why 3GPP chooses a modified version of OFDM named *Single Carrier Frequency Division Multiple Access* (SC-FDMA) for the uplink, [20].

SC-FDMA is a multiple access technique that uses the modulation scheme named *Single-Carrier Frequency-Division Multiplexing* (SC-FDM). According to, [22], its evaluation for the PAPR, gives a PAPR 2.2 dB higher for OFDM than for SC-FDM, with 100 MHz bandwidth configurations and 16-QAM as modulation scheme.

The difference with OFDM is that before the IFFT operation on the modulation symbols the FFT is performed, it would be seen as a pre-coded OFDM. In this scheme all the subcarriers are modulated by all modulation symbols, ei, although the overall transmission bandwidth is split into several subcarriers all these are modulated by the same symbol, so in a SC-FDMA symbol time, M complex subsymbols are transmitted in serial way, while a OFDM symbol although its duration is the same its transmission is in parallel way as shown in Figure 2.13, [22], [10] and [23].

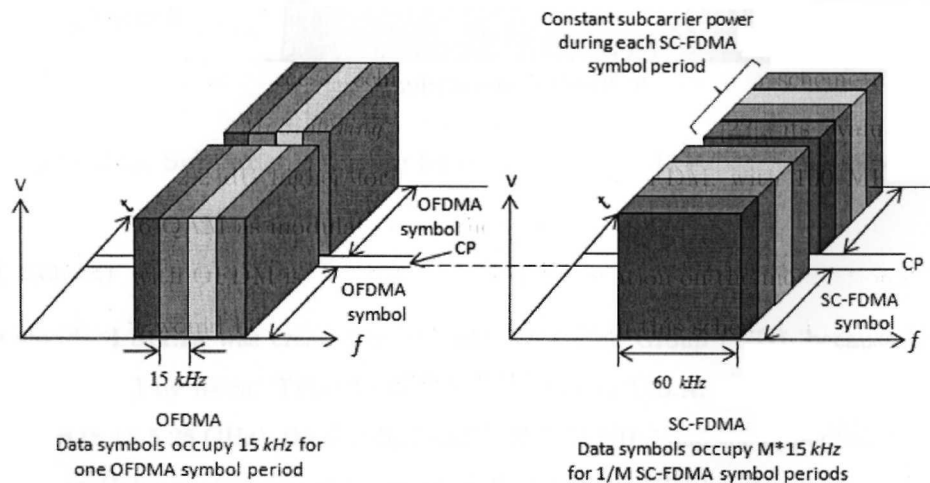


Figure 2.13: Difference between the transmission of an OFDM symbol and an SC-FDMA symbol, [23].

From the Figure 2.13 we can observe that M subsymbols are transmitted in SC-FDMA, so the envelope resulting of the signal is constant giving a peak to average power ratio lower than that of OFDM and therefore an appearance of a single-carrier can be obtained. Furthermore from channel frequency selectivity can be obtained advantage, as the symbols are in all subcarriers and although some of them are in deep fading, the information can be recover from those that have better channel conditions, [22].

Resource allocation

We had already talked about OFDMA but we have not explained how the subcarriers are grouped into resource blocks, which will be allocated to the users. The configuration in SC-FDMA for the transmission bandwidth is the same as to OFDMA, the same channel spacing, the number of subcarriers and the number of resource blocks. Subcarriers allocation can be done into two ways the *distributed* and *localized* as OFDM too.

In distributed manner when the subcarriers are equidistant it will be referred as *Interleaved* (I-FDMA), while for the localized manner the subcarrier are adjacent as depicted in Figure 2.14. Since the wireless communication is a multi-user scenario we have to choose the best option to do the resource block allocation among all users. Both have benefits, but the most common strategy is to use L-FDMA because according to, [22], [24] and [25], it offers better PAPR characteristics than I-FDMA, its gain is about 2.7 dB.

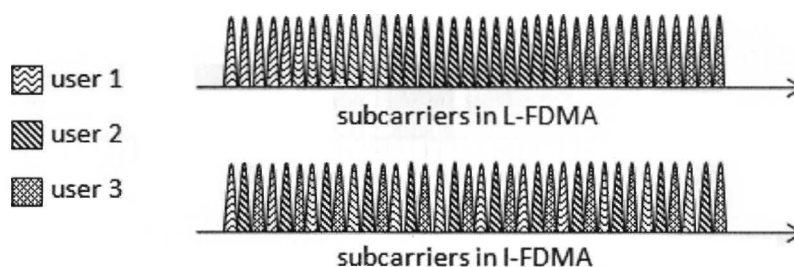


Figure 2.14: Subcarrier allocation for three users with 12 subcarriers each one.

WiFi5 (811.2a)

The standard 811.2a was created by the 811.2 Working Group (WG), because higher data rates were requested by users. This standard for example in U.S.A. uses three frequency bands, the lower band (5.15-5.25 GHz), the middle band (5.25-5.35 GHz) and the upper band (5.725-5.825 GHz) called the *Unlicensed National Information Structure* (U-NII) bands, which are less crowded, with a total bandwidth of 300 MHz. The transmit power is 40, 200 and 800mW, for the lower, middle and upper band, respectively, [11].

Since the bandwidth is fixed, the T_s have to be calculated taking into account the delay spread τ_m that range typically from 40 to 200 ns in indoor transmission whereas for outdoor environments ranges from 1 to 20 μs , [26], so the cyclic prefix is chosen following a guideline that says it should be two or four times the average delay spread. Normally, most systems add a margin for error to the delay spread, so for 802.11a has been selected a cyclic prefix of 800ns and the symbol time is four times the cyclic prefix, ie, 4 μs , [27].

The number of subcarriers established in WiFi5 are 64. Each operating channel has a $BW = 20MHz$, although it is divided into 64 subcarriers, only $N_{sc} = 52$ are used while the other 12 tones are null-carriers with a channel spacing of 0.3125 MHz. The tones to be modulated and transmitted are numbered from -26 to 26 as depicted in Figure 2.15, but that with number zero is no used because of signal processing and the tones $-27, -7, 7,$ and 21 are used as pilot symbols, so the 48 subcarriers remaining will be used to transmit data, [11], [27].

On modulation scheme to be used will depend on channel condition, among them are BPSK, QPSK, 16-QAM or 64-QAM. The coding rate will choose according to the requested data rate, 802.11a uses a convolutional encoder with coding rates $1/2, 2/3$ or $3/4$. Finally the data rates provided are 6, 9, 12, 18, 24, 36, 48 and 54 Mbps, [11].

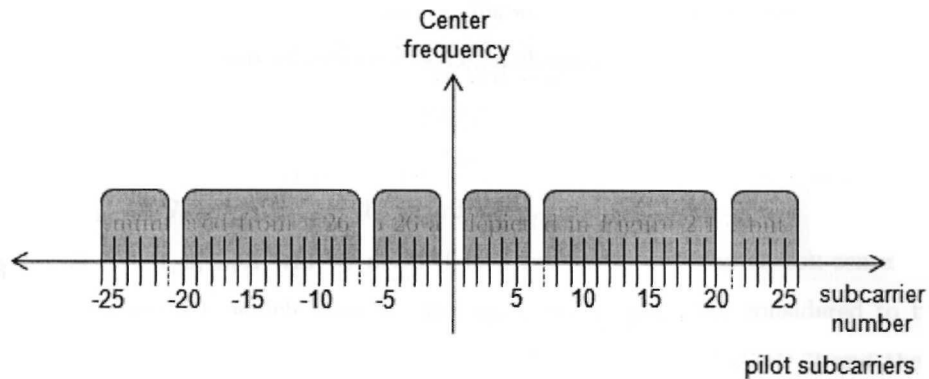


Figure 2.15: Division of a OFDM channel in WiFi5, [27].

Chapter 3

Model Description

This chapter contains the mathematical derivation of the model that describes the capacity sharing of the system, its structure and the decision rules of the model for such sharing.

3.1 Model for resource allocation

In this section, we describe the OFDM system, resource use modeling, the user's arrival process, the basic assumptions, as well as mathematical notation. The cell occupancy when there are more than one service has been introduced, in [2] and [1], in the former is analyzed the implied costs for Multirate Wireless Networks, but for this work the effect of OFDM is considered when the resources are allocated in sets of subcarriers, i.e., a channel or resource block is a set of subcarriers.

To exemplify, consider a cellular network with L hexagonal cells, with available *bandwidth* BW_i that can take values as $i = 10, 15, 20MHz$, and effective bandwidth is $BW_E = BW_i - 0.1BW_i = BW_i - BG$, where BG is the guard band.

Each cell $l = 1, 2, \dots, L$ will be divided into two areas denoted as cell-center (c) and cell-edge (e), see Figure 3.1, which have u_{lc} and u_{le} users, respectively considered to be uniformly distributed. The area of each hexagonal cell of radius R is $A_c = 3\sqrt{3}R^2/2$ and the area of the circular region of radius r is $A_0 = \pi r^2 = \pi(qR)^2$, where q is a proportion factor of the circle radius, so the proportion of area that represents the circular region, see Figure 3.1, is given by

$$P_A = \frac{A_0}{A_c} = \frac{\pi(qR)^2}{3\sqrt{3}R^2/2} = \frac{2\pi}{3\sqrt{3}}q^2. \quad (3.1)$$

BW_E is divided into two parts, one for the cell-center (BW_c) and the other for the cell-edge (BW_e). The former is assigned to the center of each of the L cells, and the latter is subdivided, but now into three parts, one part is assigned to the cell-edge of three non adjacent cells, this is repeated with another subdivision, and the remaining is assigned using the soft frequency reuse scheme. See Figure 3.2, where center of cells 1, 3 and 4 is assigned block A and the edge is assigned block B, C and D, respectively. The same assignment is done for the remaining cells.

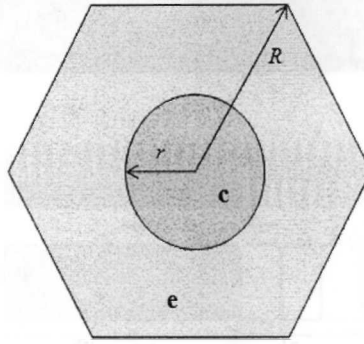


Figure 3.1: Circle area proportion

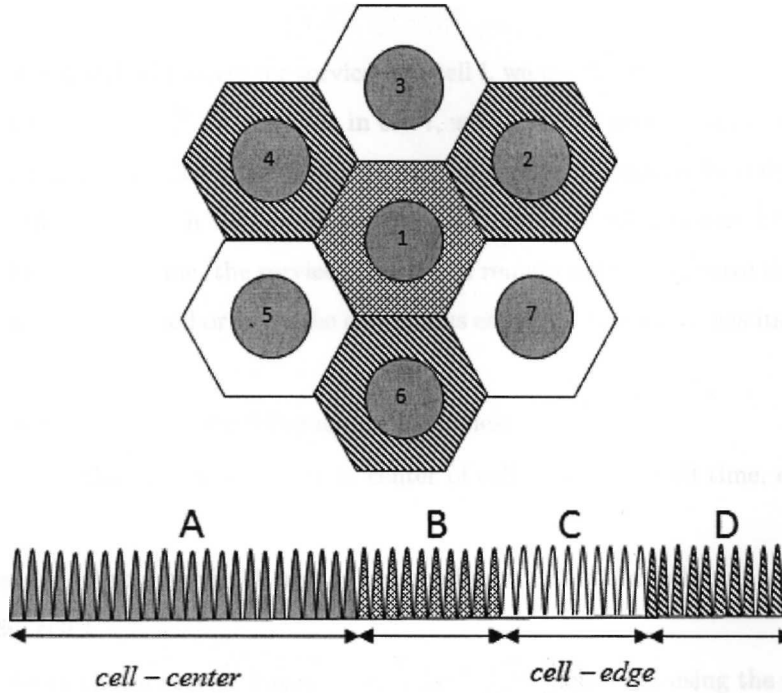


Figure 3.2: Seven-cell hexagonal system with soft frequency reuse scheme

As mentioned in the previous chapter, OFDMA divides the overall bandwidth into narrower bandwidth subcarriers, so BW_E is divided into N_{sc} (total number of subcarriers) with channel spacing Δ_f . Then, they are grouped into resource blocks, there will be N_{RB} (number of resource blocks) for each cell-center and cell-edge, see Figure 3.3, so the total number of resource blocks will be the capacity C_{le} for cell l in the edge area and C_{lc} for cell l in the center area. Let A_l be the cells adjacent to cell l . Each user will be allocated a subcarrier or a resource block as minimum resource, it depends on the service requested. We consider s types of services in each area at each cell with b_k as the bandwidth required for service $k = 1, 2, \dots, s$.

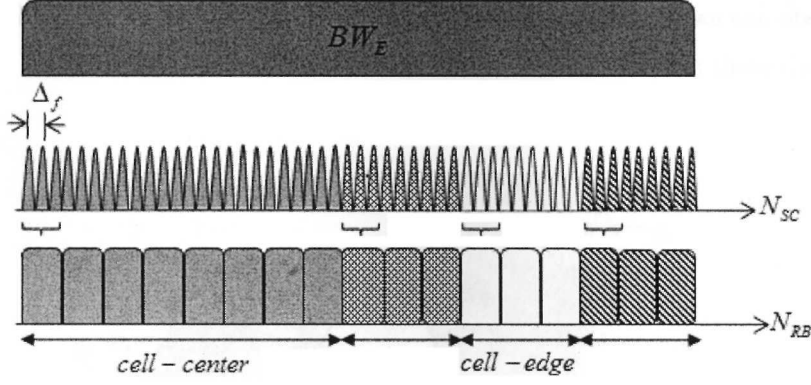


Figure 3.3: Resource blocks as capacity for center and edge area of each cell.

For the new call arrival process for service k to cell l , we use the Poisson process with rate $\lambda_{lc}^{(k)}$ for the center in cell l and $\lambda_{le}^{(k)}$ for the edge in cell l , where arrival process is independent of other new call arrival processes. The time that a requested service k remains in $\text{cell}(l, c)$ or $\text{cell}(l, e)$, is known as dwell time, which has an exponential distribution, with means $1/\mu_{lc}^{(k)}$ and $1/\mu_{le}^{(k)}$, respectively. After a dwell time, the service request can remain in the cell, leave the network, go to an adjacent area within the cell or go to the contiguous cell area, each event has its own probability to occur.

In the cell-center we have the following probabilities:

$q_{lcT}^{(k)}$ probability that a service k user in center of cell l , after a dwell time, departs from the network.

$q_{lcel}^{(k)}$ probability that a service k user in center of cell l , after a dwell time, moves to the edge area of the same cell l .

$q_{lccl}^{(k)}$ probability that a service k user, after a dwell time, continues using the same resource in the center area of cell l .

In the edge area after a dwell time, we have the following probabilities too

$q_{leT}^{(k)}$ probability that a service k user in edge of cell l , after a dwell time, departs from the network.

$q_{lecl}^{(k)}$ probability that a service k user in edge of cell l , after a dwell time, moves to the center area of the same cell l .

$q_{leem}^{(k)}$ probability that a service k user in the edge of cell l , after a dwell time, moves to the edge area of the cell m .

$q_{leel}^{(k)}$ probability that a service k user, after a dwell time, continues using the same resource in the edge area of cell l .

To exemplify this, Figure 3.4 shows a network of three cells, where we can observe the interaction between each cell after a dwell time, where the probabilities are as those described before.

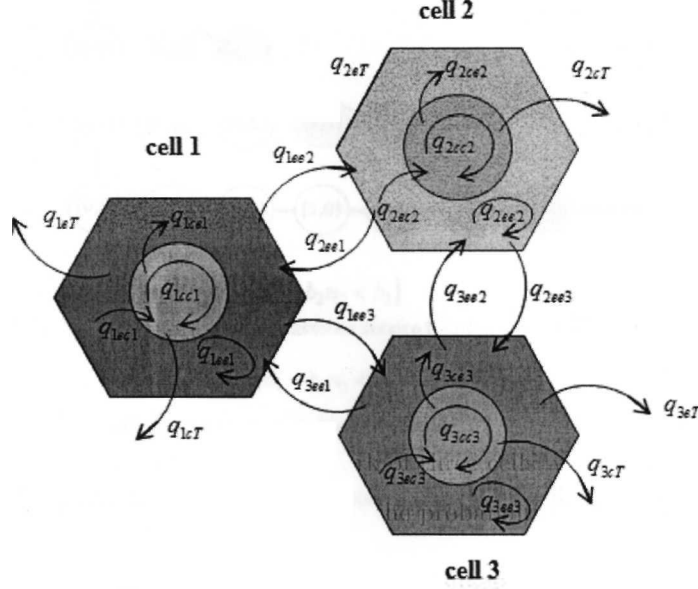


Figure 3.4: Three-cell hexagonal system with interaction between them.

The total sum of the probabilities in each area must be one. As follows, for the center of each cell l we have

$$q_{lcc}^{(k)} + q_{leT}^{(k)} + q_{lcc}^{(k)} = 1, \quad (3.2)$$

and for the edge of each cell l

$$q_{leT}^{(k)} + q_{lecl}^{(k)} + q_{leel}^{(k)} + \sum_{m \in A_l} q_{leem}^{(k)} = 1. \quad (3.3)$$

We assume that cell occupancy evolves according to an s -dimensional birth-death process independent of other cells. To obtain the s -dimensional Markov chain, we first establish the following, let $\Omega(C)$ be the space of feasible states, i.e., $\Omega(C) = \{\underline{n} : C - \sum_{k=1}^s n_k b_k \geq 0\}$, where $\underline{n} = (n_1, n_2, \dots, n_s)$ is the state of the area center or edge at cell l with \mathbf{n}_k being the active number of service k sessions. Let $\Psi_{la}^{(k)}$, where a can be center (c) or edge (e) area of cell l , be the set of blocked states for traffic class k , i.e. $\Psi_{la}^{(k)} = \{\underline{n} : C - \sum_{k=1}^s n_k b_k < b_k\}$. These statements can be understood as established in Figure 3.5.

We assume that the total offered traffic is given by $\rho_{la}^{(k)} = \lambda_{la}^{(k)} + \beta_{la}^{(k)}$, where $\lambda_{la}^{(k)}$ is the offered traffic to area a of the cell l and $\beta_{la}^{(k)}$ is the term for the handoffs offered traffic from adjacent areas and cells. Finally, the rate of departure of a state \mathbf{n}_k of service type k of the area a from cell l is given by $n_k \mu_{la}^{(k)} (1 - q_{aa,l}^{(k)})$, i.e., n_k is the state that is left, $\mu_{la}^{(k)}$ is the rate and $1 - q_{aa,l}^{(k)}$ is the

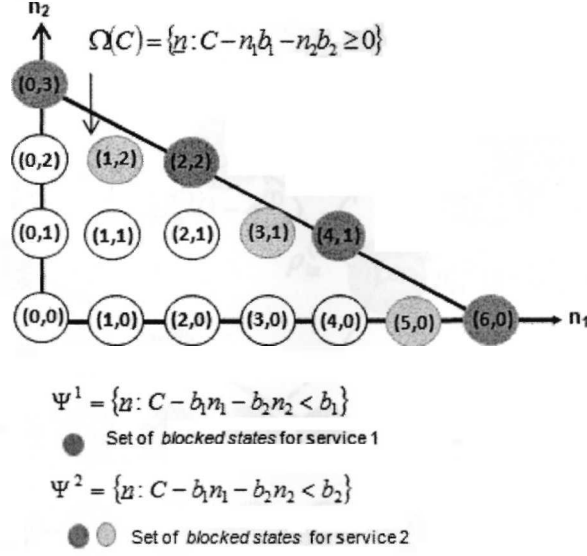


Figure 3.5: Birth-death process of a cell with $s=2$, $C=6$, $b_1 = 1$ and $b_2 = 3$.

likelihood of occurring the event. So to get the stationary distribution of the s -dimensional Markov chain of cell l , we establish the global balance equations, where we use the normalization given by $\sum_{(n_1, \dots, n_s) \in \Omega(C)} P_{la}(\underline{n}) = 1$. The equation (3.4) gives that probability and Figure 3.6 shows a 2-dimensional birth death process in a cell.

$$P_{la}(\underline{n}) = \left[\sum_{k=1}^s \rho_{la}^{(k)} + \sum_{k=1}^s n_k \mu_{la}^{(k)} (1 - q_{aa,l}^{(k)}) \right]^{-1} \left[\sum_{k=1}^s \rho_{la}^{(k)} P_{la}(\underline{n}_k^-) + \sum_{k=1}^s (n_k + 1) \mu_{la}^{(k)} (1 - q_{aa,l}^{(k)}) P_{la}(\underline{n}_k^+) \right]. \quad (3.4)$$

where $\underline{n}_k^+ = (n_1, n_2, \dots, n_{k-1}, n_k + 1, n_{k+1}, \dots, n_s)$ and $\underline{n}_k^- = (n_1, n_2, \dots, n_{k-1}, n_k - 1, n_{k+1}, \dots, n_s)$. Having obtained the probability of being in state \underline{n} , in area a at cell l we calculate the blocking probability of a new request of service k , given by

$$B_{la}^{(k)} = \sum_{n \in \Psi_{la}^{(k)}} P_{n,la}^{(k)}. \quad (3.5)$$

As mentioned $\beta_{la}^{(k)}$ is the offered handoff traffic, in other words, the requests of service k that originate at area a that were accepted, and that go to other area of the same cell, or go to the area of other cell with its respective probability, i.e., $\rho_{le}^{(k)}(1 - B_{le}^{(k)})q_{lecl}^{(k)}$, $\rho_{lc}^{(k)}(1 - B_{lc}^{(k)})q_{lcel}^{(k)}$. So the handoff rate for cell-center and cell-edge are

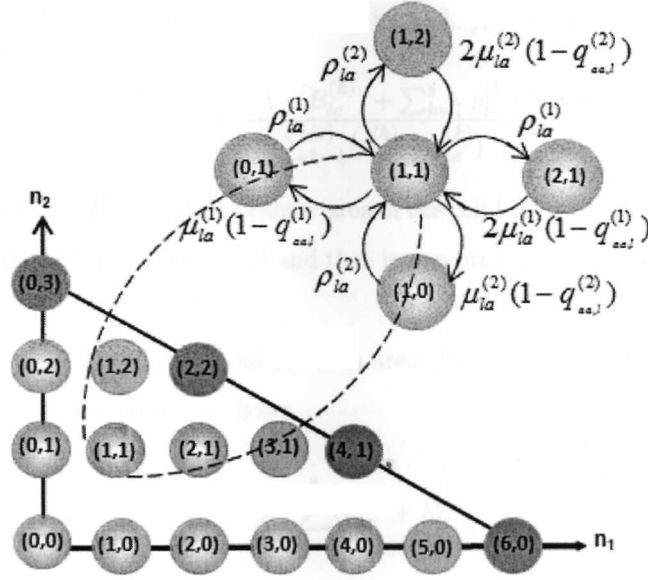


Figure 3.6: 2-dimensional birth-death process with $C=6$, $b_1 = 1$ and $b_2 = 3$.

$$\beta_{lc}^{(k)} = \rho_{le}^{(k)}(1 - B_{le}^{(k)})q_{lecl}^{(k)}, \quad (3.6)$$

$$\beta_{le}^{(k)} = \rho_{lc}^{(k)}(1 - B_{lc}^{(k)})q_{lecl}^{(k)} + \sum_{m \in A_l} \rho_{me}^{(k)}(1 - B_{me}^{(k)})q_{meel}^{(k)}. \quad (3.7)$$

Using Equation (3.6) the total offered traffic for center area of cell l is given by

$$\rho_{lc}^{(k)} = \lambda_{lc}^{(k)} + \rho_{le}^{(k)}(1 - B_{le}^{(k)})q_{lecl}^{(k)}, \quad (3.8)$$

and using Equation (3.7), the total offered traffic for the edge area is

$$\rho_{le}^{(k)} = \lambda_{lc}^{(k)} + \rho_{lc}^{(k)}(1 - B_{lc}^{(k)})q_{lecl}^{(k)} + \sum_{m \in A_l} \rho_{me}^{(k)}(1 - B_{me}^{(k)})q_{meel}^{(k)}. \quad (3.9)$$

The total offered traffic to center area of each cell using Equation (3.8) can be calculated as:

$$\rho_{lc} = \sum_{k=1}^{(s)} \rho_{lc}^{(k)}, \quad (3.10)$$

and using equation (3.9) the total offered traffic for the edge area of a cell is given by

$$\rho_{le} = \sum_{k=1}^{(s)} \rho_{le}^{(k)}, \quad (3.11)$$

To calculate the blocking of a cell we use equations (3.5), (3.8) and (3.9) as follows

$$B_l = 1 - \frac{\sum_{k=1}^s \rho_{lc}^{(k)} (1 - B_{lc}^{(k)}) + \sum_{k=1}^s \rho_{le}^{(k)} (1 - B_{le}^{(k)})}{\sum_{k=1}^{(s)} (\rho_{lc}^{(k)} + \rho_{le}^{(k)})}. \quad (3.12)$$

where $\rho_{lc}^{(k)}(1 - B_{lc}^{(k)})$ is the offered traffic to center area of the cell l and that is accepted, $\rho_{le}^{(k)}(1 - B_{le}^{(k)})$ is the offered traffic to edge area of the cell l and that is accepted, and $\rho_{lc}^{(k)} + \rho_{le}^{(k)}$ is the total offered traffic to cell l .

Until now we have presented equations for each area of a cell, but to calculate the total offered traffic to the network we derived it as follows

$$\lambda_T = \sum_l \sum_{k=1}^s (\lambda_{lc}^{(k)} + \lambda_{le}^{(k)}), \quad (3.13)$$

The blocking probability that is seen by a new user that requests a service k anywhere in the network, i.e., the network blocking is calculated as

$$B_T = 1 - \frac{\sum_l \sum_{k=1}^s (\lambda_{lc}^{(k)} + \lambda_{le}^{(k)}) (1 - B_l)}{\lambda_T}. \quad (3.14)$$

3.2 Model for channel-aware resource allocation.

In the previous section the mathematical derivation of the model used for the allocation of resources in a system, channel conditions were not being taken into account. In this section, we do include channel conditions, so the model will change a little as shown below.

For wireless communications the transmission medium is a radio channel, this has the property that the bit error probability rate or the signal to noise ratio is varying in time, so this type of channel are called time-variant channel. There are models that focus only on the distribution of the receiver amplitude and the time-dependent correlation behavior of the channel, i.e., the channel memory. The model for our simulation with that characteristics is the channel model of Gilbert-Elliot, [28], which is applicable to describe a digital communication channel. This describes the time periods when the signal is degraded, and it is given by a 2-state Markov chain. The wireless channel can be only in two states, the state space is $\Omega = \{good, bad\}$. The time that channels remain in the *good* state has exponential distribution with mean $1/\gamma$, after which it goes to the *bad* state to transmit and its duration period has exponential distribution too, but with mean $1/\kappa$. When a user has requested a k service it is assumed that when he is in the *good* state of the channel there will not be errors, but if the channel is in the *bad* state then the user may not complete its session. A diagram that shows how a channel of a user is, is depicted in Figure 3.7, the session

total duration is denoted as t_s , with $t_i = 0$ as the time when the session initialized. After that, the channel go to the *good* state of wireless channel or to the *bad* state and so on. The t_s can be divided into cycles, where the channel in each cycle is in the *good* and then in the *bad* state of the wireless channel, with a time duration of $t_{g,i}$ and $t_{b,i}$, respectively, where i is the i -th cycle, [28].

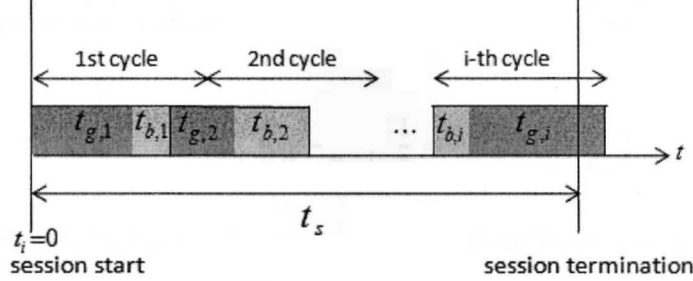


Figure 3.7: Description of the evolution of a lossy channel in a wireless network.

For our system the Markov chain is depicted in Figure 3.8, where γ is the rate at which a subcarrier goes from the good to bad state and κ represents the reverse situation.

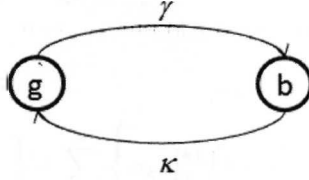


Figure 3.8: 2-state Markov chain that describes a digital communication channel.

Recall that each resource block is a set of three subcarriers and assume that a *RB* is in the *bad* state of the channel if two of the subcarriers are in that condition. If we are in a state of the 3-dimensional Markov chain and we focus on service 1 of area e at cell l of the network, we establish that if a *RB* that is in the bad state of the channel changes to the good state of the channel then that *RB* leaves that unavailable state and now is in an available state. For this we have for the service 1

$$\sum_{j=0}^{n_1} \left\{ \kappa 3(n_1 - j) \left(\frac{1}{n_1 - j} \right)^2 \frac{1}{6} \right\} = \sum_{j=0}^{n_1} \left\{ \kappa \frac{1}{2} \left(\frac{1}{n_1 - j} \right) \right\}, \quad (3.15)$$

where

3: number of subcarrier of a resource block

κ : rate for go from a bad state to a good state

j is the j -th resource block that is busy,

n_1 : unavailable resource blocks,

$n_1 - j$: resources blocks that are in the *bad* state.

So the channels (RBs) can be available when a user ends his service session and when a channel changes from bad to a good condition. The occupation of the resources arises when a new user requests a service k and when a channel in good channel condition goes to a bad condition, then the total offered traffic is affected with the following term that describes the last situation

$$(RB - n_1) \gamma 3 \left(\frac{1}{RB - n_1} \right)^2 \frac{1}{6} = \gamma \frac{1}{2} \left(\frac{1}{RB - n_1} \right). \quad (3.16)$$

where 3 is the number of subcarrier of a resource block, γ is the rate for go from a good state to a bad state and n_1 is the number of blocks. Recall that occupancy of a resource block can be only when a user of class k service has arrived or when the channel is in the good state and goes to the bad state, but only a event occurs in a interval of time. To describe the influence of the channel conditions on the stationary distribution of the s -dimensional Markov chain, see Figure 3.9 , we take Equation (3.4) and add the terms given by equations (3.15) and (3.16) as follows

$$P_{la}(\underline{n}) = \left[\sum_{k=1}^s \left\{ \rho_{la}^{(k)} + \gamma \frac{1}{2} \frac{1}{RB - n_k} \right\} + \sum_{k=1}^s \left\{ n_k \mu_{la}^{(k)} (1 - q_{aa,l}^{(k)}) + \sum_{j=0}^{n_k} \left\{ \kappa \frac{1}{2} \left(\frac{1}{n_k - j} \right) \right\} \right\} \right]^{-1} \left[\sum_{k=1}^s \rho_{la}^{(k)} P_{la}(\underline{n}_k^-) + \sum_{k=1}^s (n_k + 1) \mu_{la}^{(k)} (1 - q_{aa,l}^{(k)}) P_{la}(\underline{n}_k^+) \right] \quad (3.17)$$

The calculation of blocking probability for a new request of service k remains the same as that of Equation (3.5), since $P_{\underline{n},la}^{(k)}$ already contains the modification due to the channel condition. But we have to mention that now the offered traffic have to be calculated for each state of each service at center and edge area of a cell, because the channel conditions now are influencing the occupancy of the channels. To derive the total offered traffic for each state of the s -dimensional Markov chain for center and edge area at each cell we define $\underline{n}_{la} = (n_{la}^{(1)}, n_{la}^{(2)}, \dots, n_{la}^{(k)}, \dots, n_{la}^{(s)})$ with a as c or e depending on the area, then the total offered traffic for the center area is calculated as follows

$$\rho_{lc}^{(k)}(\underline{n}_{lc}) = \lambda_{lc}^{(k)} + \gamma \frac{1}{2} \left(\frac{1}{RB_k - \underline{n}_{lc}} \right) + \sum_{\underline{n}_{le}=0}^{RB_{le}^{(k)}-1} \rho_{le}^{(k)}(\underline{n}_{le}) (1 - B_{le}^{(k)}) q_{lecl}^{(k)} \tilde{P}_{le}(\underline{n}_{le}), \quad (3.18)$$

and for the edge area

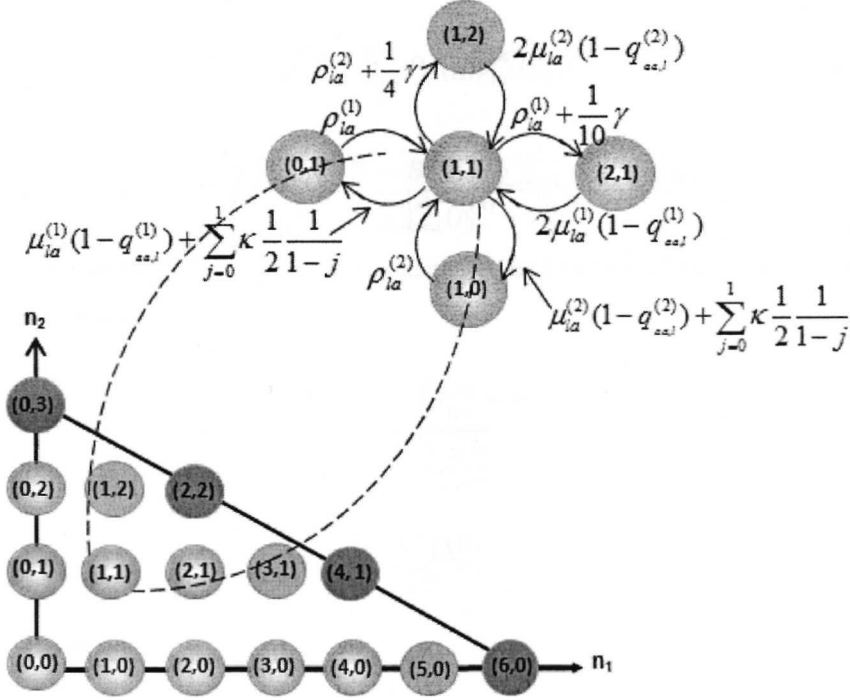


Figure 3.9: 2-dimensional birth-death process with $RB_1 = 6$, $RB_2 = 3$, $n_1 = 1$ and $n_2 = 2$.

$$\begin{aligned}
 \rho_{le}^{(k)}(n_{le}) &= \lambda_{le}^{(k)} + \gamma \frac{1}{2} \left(\frac{1}{RB_{le}^{(k)} - n_{le}^{(k)}} \right) + \sum_{n_{lc}=0}^{RB_{lc}^{(k)}-1} \rho_{lc}^{(k)}(n_{lc}) (1 - B_{lc}^{(k)}) q_{lcel}^{(k)} \tilde{P}_{lc}(n_{lc}) \\
 &\quad + \sum_{m \in A_l} \sum_{n_{me}=0}^{RB_{me}^{(k)}} \rho_{me}^{(k)}(n_{me}) (1 - B_{me}^{(k)}) q_{meel}^{(k)} \tilde{P}_{me}(n_{me}). \quad (3.19)
 \end{aligned}$$

where $n_{lc}^{(k)} = 0, 1, 2, \dots, RB_{lc}^{(k)} - 1$ and $n_{le}^{(k)} = 0, 1, 2, \dots, RB_{le}^{(k)} - 1$. The expressions to calculate the probability to be at state n with service k in the center or edge area of the cell l denoted as $\tilde{P}_{le}(n_{le})$ and $\tilde{P}_{lc}(n_{lc})$ are given by considering a specific constant value of $n_{lc}^{(k)}$ and $n_{le}^{(k)}$, respectively, as follows

$$\tilde{P}_{le}(n_{le}) = \sum_{\underline{n}: n_{le}^{(k)} = \text{constant}} P_{le}(\underline{n}), \quad (3.20)$$

$$\tilde{P}_{lc}(n_{lc}) = \sum_{\underline{n}: n_{lc}^{(k)} = \text{constant}} P_{lc}(\underline{n}). \quad (3.21)$$

Now to obtain the blocking of a cell we derive the equations to the total offered traffic to wherever area of a cell as

$$\rho_{la}^{(k)} = \sum_{\underline{n}} P_{la}(\underline{n}) \rho_{la}^{(k)}(\underline{n}_{la}) \quad (3.22)$$

$$\tilde{B}_l = 1 - \frac{\sum_{k=1}^s \rho_{lc}^{(k)} (1 - B_{lc}^{(k)}) + \sum_{k=1}^s \rho_{le}^{(k)} (1 - B_{le}^{(k)})}{\sum_{k=1}^s (\rho_{lc}^{(k)} + \rho_{le}^{(k)})}. \quad (3.23)$$

Since we have derived the expression to calculate the blocking of the cells, we can obtain the blocking of the network as follows

$$\tilde{B}_T = 1 - \frac{\sum_l \sum_{k=1}^s (\lambda_{lc}^{(k)} + \lambda_{le}^{(k)}) (1 - \tilde{B}_l)}{\lambda_T}. \quad (3.24)$$

where

$$\lambda_T = \sum_l \sum_{k=1}^s (\lambda_{lc}^{(k)} + \lambda_{le}^{(k)}). \quad (3.25)$$

3.2.1 Net Revenue

A measurement of performance in a wireless network is the Net Revenue W , that is the revenue that is generated when the traffic has been carried successfully, [2]. This revenue take into account two concepts, first one generates a revenue $w_{la}^{(k)}$ when the offered traffic of service k to cell-center or cell-edge of the cell l is accepted, i.e., $\lambda_{la}^{(k)} (1 - B_{la}^{(k)}) w_{la}$, where the last term has currency units of revenue when a user is conected. The second term contains the offered handoffs of service k that have been offered to center area or edge area of cell l are blocked and those channels unavailable because of interference and the outage in the area of a cell that causes loss for unsuccessful call and services that are not completed with a cost of $z_{la}^{(c)}$. Hence the net revenue is calculated as follows

$$W = \sum_l \sum_a \sum_k \lambda_{la}^{(k)} (1 - B_{la}^{(k)}) w_{la}^{(k)} - \sum_l \sum_a \sum_k [\rho_{la}^{(k)} - \lambda_{la}^{(k)}] B_{la}^{(k)} z_{la}^{(k)} \quad (3.26)$$

where $B_{la}^{(k)}$ is the blocking probability of service k of the center or edge area at cell l .

Basic assumptions

- The number of resource blocks to each user depends on the service type
- When a handoff arises, the number of resource blocks that a user is using will be the same in the following area. The handoff, can be intra handoff or inter handoff.
- To consider a resource block in bad condition two of the three subcarries of the RB has to be inthe bad state.

Chapter 4

Numerical Results

This chapter presents numerical results of the blocking probability by solving the model proposed in Chapter 3 for a network of three cells with three services each one given by a 3-dimensional Markov chain and the revenue of the network.

Results are given for two sceneries:

- The model is evaluated regardless of channel conditions for the allocation of block resources.
- The solution of the model take into account the conditions of channel, i.e. not only is consider if there are resources to be allocated but also if the channel has good or bad conditions.

In both scenarios presented the same levels of mobility are used, but in the case of the net revenue the mobility changes to be higher in order to see how it affects performance.

As it was mentioned earlier after a dwell time some events arise like if the user that requested a service continues using the resources, ends their request, or go to other area. So, we consider that there is mobility when the user go to another area or cell, for each case the probabilities were calculated, where the likelihood of leaving the resources for each service was fixed as well as that to stay with the resources in the same area of each cell. Since the total likelihood must be 1, we assume for the edge of a cell that the probability to go to the center of that cell is the same of going to the edge of other cell. Equations obtained are

$$q_{lcel}^{(s)} = 1 - q_{lcT}^{(s)} - q_{lccl}^{(s)} \quad (4.1)$$

$$q_{leem}^{(s)} = 1 - q_{leT}^{(s)} - q_{lecl}^{(s)} - q_{leel}^{(s)}. \quad (4.2)$$

Other consideration is presented when there is no mobility, i.e.

$$q_{lcT}^{(s)} + q_{lccl}^{(s)} = 1 \quad (4.3)$$

$$q_{leT}^{(s)} + q_{leel}^{(s)} = 1. \quad (4.4)$$

4.1 Resource allocation in OFDM systems regardless channel conditions

This section studies channel availability, therefore the blocking probability returns information about how the resources are being occupied when the new service request arrival rate is growing. The scenario is a 3-cell network, where each cell has a center and edge area as well as three types of services $s = 3$, see Figure 4.1. The effective bandwidth is $BW_E = 2.7MHz$, this was taken from Table 2.1 where are included the ranges of bandwidth for LTE. This narrow bandwidth enables a smooth transition to the spectrum of precedent mobile systems, [29]. With $2.7MHz$ the raw rate is of 16.2Mbps when the scheme of Modulation is 64 QAM. Now the BW_E is divided into subcarriers where the channel spacing is $\Delta_f = 15kHz$ and the total number of subcarriers are $N_{sc} = 2.7MHz/15kHz = 180$.

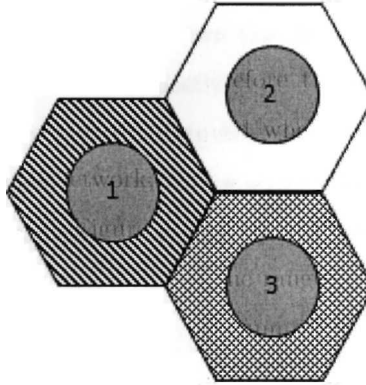


Figure 4.1: 3-cell hexagonal network.

Number of subcarriers for center and edge area is calculated as $N_{sc,c} = 180/2 = 90$ and $N_{sc,e} = 180/6 = 30$, respectively, but the resource is given in sets of three subcarriers so the number of resource blocks for each area is $N_{RB,c} = 90/3 = 30$ and $N_{RB,e} = 30/3 = 10$. The center area of each cell has the same resource blocks, whereas the edge of each cell has different resource blocks, see Figure 4.2. The bandwidth requirements in resource blocks for services type 1, 2 and 3 are $b_1 = 1$, $b_2 = 2$ and $b_3 = 5$ respectively in both areas of each cell, because if a user requested the service 1, 2 or 3, and goes to other area he will be using the same capacity.

The new service request arrival rates, bandwidth requirements for service type 1, 2 and 3, and number of resource blocks are given in Table 4.1 where only one cell is considered, because the remainin cells are the same.

Probabilities calculated for simulation are shown in Table 4.2, where the high and low mobility

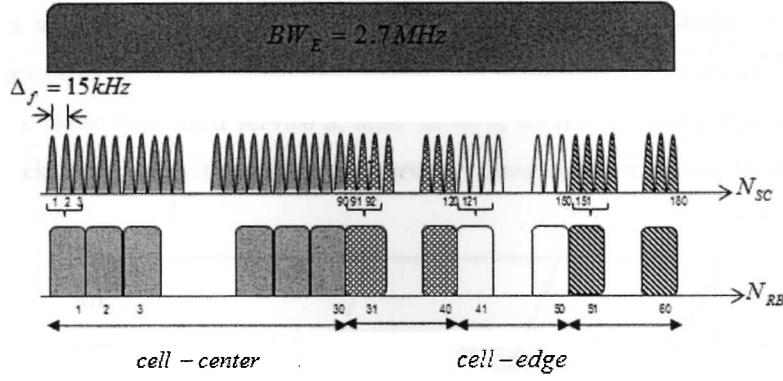


Figure 4.2: Capacity for each area at cell l .

Table 4.1: Simulation parameters

$Cell_l$	$N_{RB,l}$	$b_l^{(1)}$	$b_l^{(2)}$	$b_l^{(3)}$	$\lambda_l^{(1)}$	$\lambda_l^{(2)}$	$\lambda_l^{(3)}$	$\mu_l^{(s)}$
cell-center	30	1	2	5	5.130	2.250	1.102	1
cell-edge	10	1	2	5	0.6696	0.3298	0.1259	1

are regarded. Probabilities for q_{lcT} and q_{leT} shown that 90%, 92% y 94% of the users that were using resources of type service 1, 2 and 3 respectively will leave the network after the dwell time finishes for low mobility, whereas for high mobility decreases the percentage to 80%, 82% and 84%. Meanwhile likelihood for active users will go to other area of the same cell after that time is higher than that to go to other cells regardless of mobility.

Table 4.2: Parameters for mobility for the three cells.

Mobility	Type of service	q_{lcT}	q_{lcel}	q_{leT}	q_{lecl}	q_{leem}
Low Mobility	1	0.90	0.025	0.90	0.025	0.0125
	2	0.92	0.02	0.92	0.02	0.01
	3	0.94	0.015	0.94	0.015	0.0075
High Mobility	1	0.80	0.125	0.80	0.06	0.045
	2	0.82	0.12	0.82	0.056	0.042
	3	0.84	0.115	0.84	0.052	0.039

4.1.1 Blocking results

To obtain the results, the new service request arrival rate for all services on center area and edge area at all cells were constant except for center of cell 1 with type service 1. Figures 4.3 to 4.5 show likelihood when a service request of wherever service ends and leave the network ($q_{iT}^{(s)} = 1$). Figure 4.3 for service 1 of the center area of the cell 1 shows blocking probability that starts from 0 because its offered traffic parameter is being varied, whereas for services 2 and 3 already exist a nonzero new service request arrival rate. It is seen that service 3 has higher blocking when the arrival rate begins, this is because the resource block requirement for it is higher than that of other

ones, so when a user that need service 3 arrives, he takes 5 resource blocks, but there are still resources to meet other services. While new arrival rate is growing the users to be blocked at the beginning will be those who need service 3, after those of service 2 whose band requirements are two resource blocks and finally those that use service 1 since only a resource block is used.

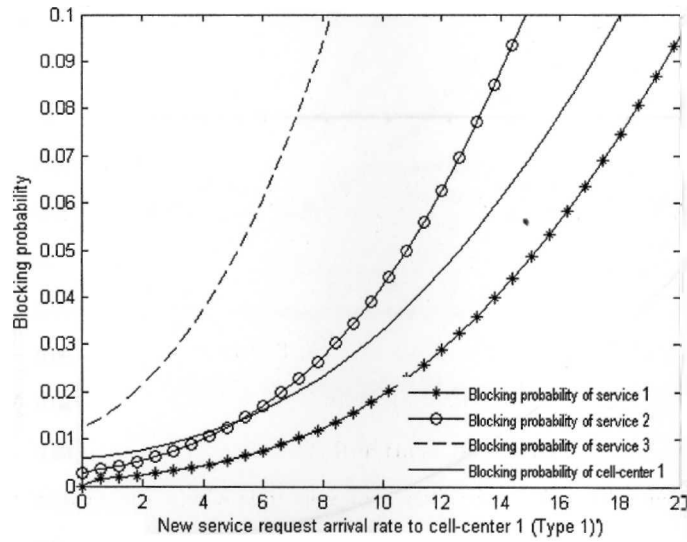


Figure 4.3: Blocking probability where is no mobility for center area of cell 1.

To users at the edge area of cell 1, blocking probabilities are higher because of resource blocks are less than those for the center area, besides in the no mobility case are constant as seen in Figure 4.4.

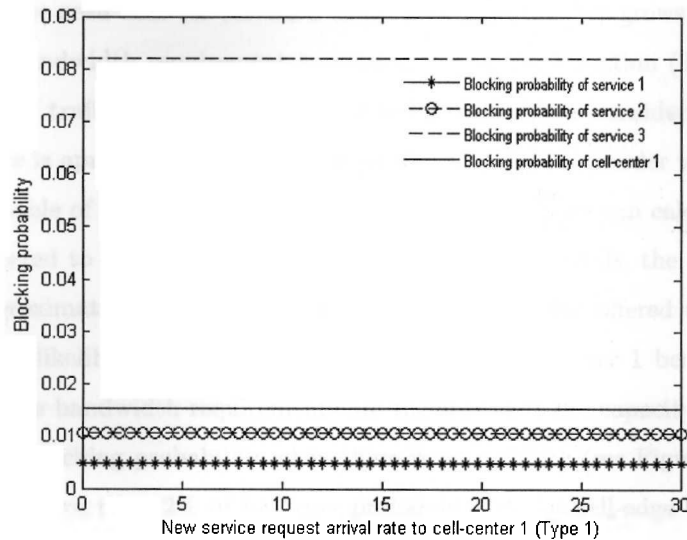


Figure 4.4: Blocking probability without mobility for edge area of cell 1.

Figure 4.5 shows network blocking probability calculated with Equation (3.14) as a function of the arrival rate. It can be seen that a network blocking is less than 2% when the new request arrival rate for cell-center 1 is approximately 9.6, for this rate we calculate it as porcentaje of the total traffic offered to network given by Equation (3.13). Then maximum offered traffic rate in that area is 28.83% of the total offered traffic to network to meet that probability.

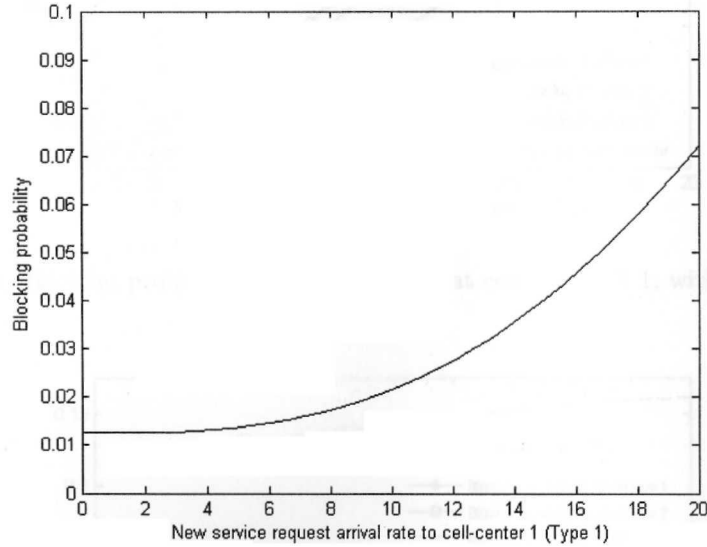


Figure 4.5: Network blocking probability without mobility, $q_{IT}^{(s)} = 1$.

For low mobility the blocking probabilities for each service at center of cell 1 are shown on Figure 4.6. It can be seen that for service 3 the blocking probability grows faster than the other ones because the bandwidth requirement is greater. Using the Equation (3.10) we can calculate the the total offered traffic to center area of the cell 1, now if it is considered that new service 1 request arrival rate is aproximately 6 as can be seen in that figure in order to be under a blocking probability acceptable of 2%, then with that request arrival rate we can calculte what percentage of ρ_{1c} is being offered to service 1 in the cell-center 1, in order words, the new service 1 request arrival rate of aproximately 6 corresponds to 63.95% of the total offered traffic to center area. For the cell-edge 1 likelihood is bigger than likelihood for cell-center 1 because (Figure 4.7), as mentioned above the bandwidth requirements are the same but the capacity is three times lower. If we compare the blocking probability when there is no mobility (see Figure 4.4) it can be seen that there will be more than 2% of blocking probability for for cell-edge 1 with the same new service request arrival rate.

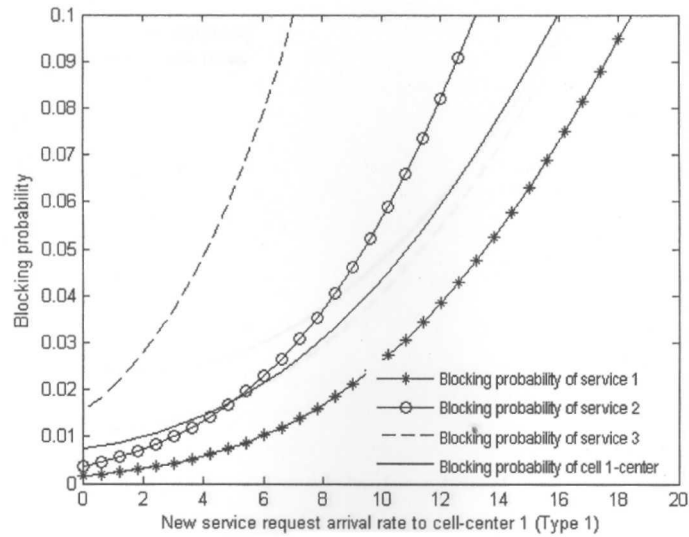


Figure 4.6: Blocking probability for each service at center of cell 1, with low mobility.

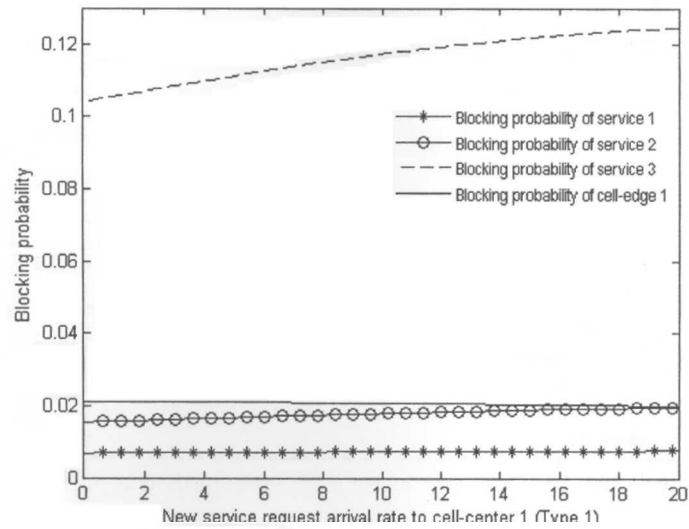


Figure 4.7: Blocking probability with low mobility for edge area of cell 1.

Now, in Figure 4.8, it is shown that new service request arrival rate has decreased slightly compared to the rate for the center of the cell, to maintain good total blocking probability in cell 1. The blocking increases when there is high mobility since the probability that a user leaves the area where he starts the service and go to an area of the same cell has grown and is greater than the probability of going to other cells (see Table 4.2). If users start to go to other cells with a higher likelihood then adjacent cells to cell 1 will experience a higher blocking as is depicted in Figure 4.9. This figure shows how blocking grows for cell 2.

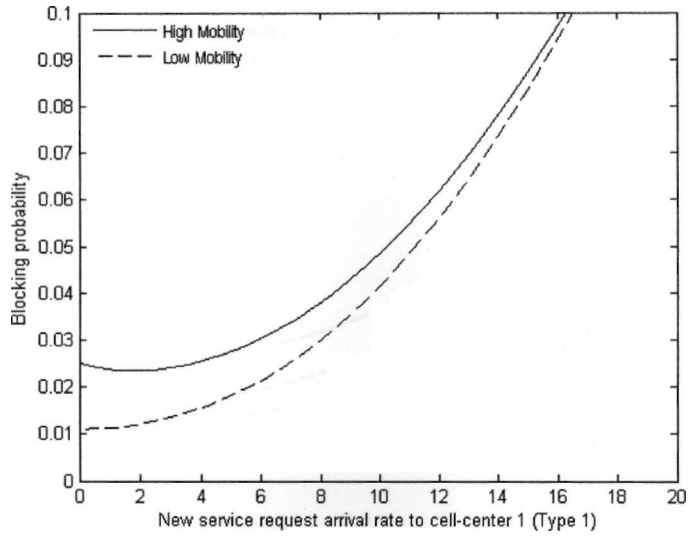


Figure 4.8: Blocking probability with low and high mobility for cell 1.

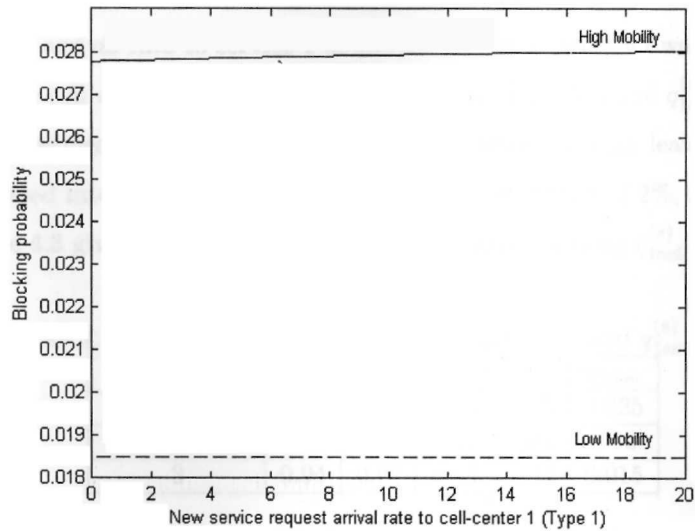


Figure 4.9: Blocking probability of cell 2 where low and high mobility is considered.

Figure 4.10 shows the comparison of the network blocking probability as a function of the arrival rate for different levels of mobility. As can be seen the grade of service of 2% is met only for no mobility and low mobility, with an offered traffic to service 1, center area at cell 1 of 28.83% and 21.78% from total offered traffic to the network, respectively. This percentage is calculated as follows, we locate the maximum value of offered traffic for service 1 to center area at cell 1 to be under that grade of service for the two levels of mobility, then we calculate them as percentage of the total offered traffic to the network that is given by the Equation (3.13).

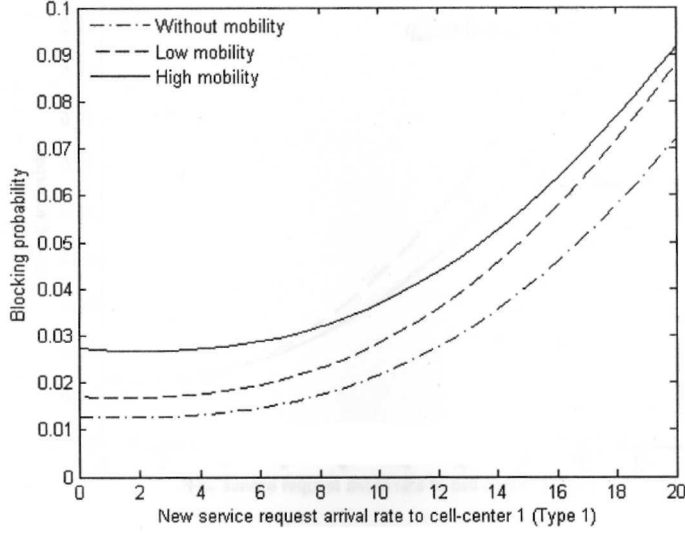


Figure 4.10: Network blocking probability with low and high mobility.

Figures 4.11 and 4.12 show the comparison of blocking probability of cell 1 and the network as a function of the arrival rate to service 1 of the cell-center 1, when a dwell time ends and users leave the area of the cell where they requested a service, i.e., $q_{1cc1}^{(s)} = 0$ and $q_{1ee1}^{(s)} = 0$. It is seen that the arrival rate to service 1 of the cell-center 1 is higher when the user leaves the area where the service was requested instead of stay there, to have a grade of service of 2%, so higher performance is obtained. Table 4.3 gives the values when mobility increases setting $q_{1cc1}^{(s)} = 0$ and $q_{1ee1}^{(s)} = 0$.

Table 4.3: Parameters for mobility with $q_{1cc1}^{(s)} = 0$ and $q_{1ee1}^{(s)} = 0$.

Type service	q_{lcT}	q_{lcl}	q_{leT}	q_{lecl}	q_{leem}
1	0.90	0.1	0.90	0.05	0.025
2	0.92	0.08	0.92	0.04	0.02
3	0.94	0.06	0.94	0.03	0.015

4.1.2 Net revenue results

As was said in chapter 3 the net revenue is a performance measurement, so for different levels of mobility it is plotted in Figure 4.13 . The revenues chosen when the request of a session of service k is accepted in the center or edge area of the cell l are shown in Table 4.4, as well as the cost when the session ends because the hand off was blocked. That figure shows that the best revenue generated is when there is no mobility or when it is low, while for the high mobility this decrease. If the mobility increases more and more, Figure 4.14 shows that revenue tends to have a maximum in a specific value of the new service arrival rate to cell-center one ($\lambda_{1c}^{(1)}$), after which

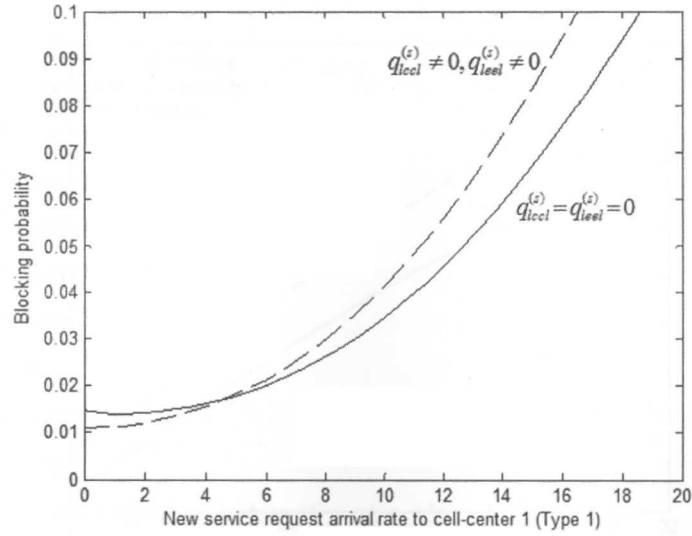


Figure 4.11: Comparison of blocking probability for cell 1, $q_{lcc1}^{(s)} \neq 0$, $q_{lee1}^{(s)} \neq 0$ and $q_{lcc1}^{(s)} = q_{lee1}^{(s)} = 0$.

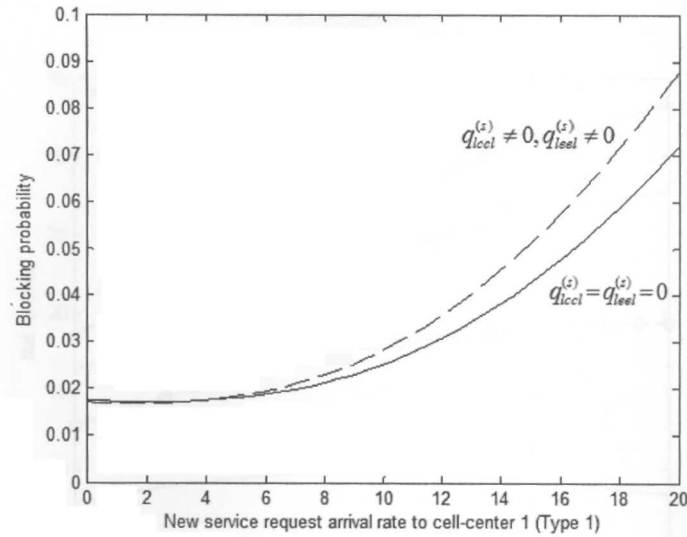


Figure 4.12: Comparison of blocking probability for the network, $q_{lcc1}^{(s)} \neq 0$, $q_{lee1}^{(s)} \neq 0$ and $q_{lcc1}^{(s)} = q_{lee1}^{(s)} = 0$.

this decreases although the arrival rate $\lambda_{1c}^{(1)}$ continues growing. For this figure it was considered the mobility for all services at each area of each cell to obtain the network mobility from Table 4.2, where the high mobility was increased about 10% each time for each curve.

Table 4.4: Parameters for net revenue.

$Cell_l$	Type service	w_{la}	z_{la}
area(cell, edge)	1	1	3
	2	0.8	1.4
	3	0.6	1.8

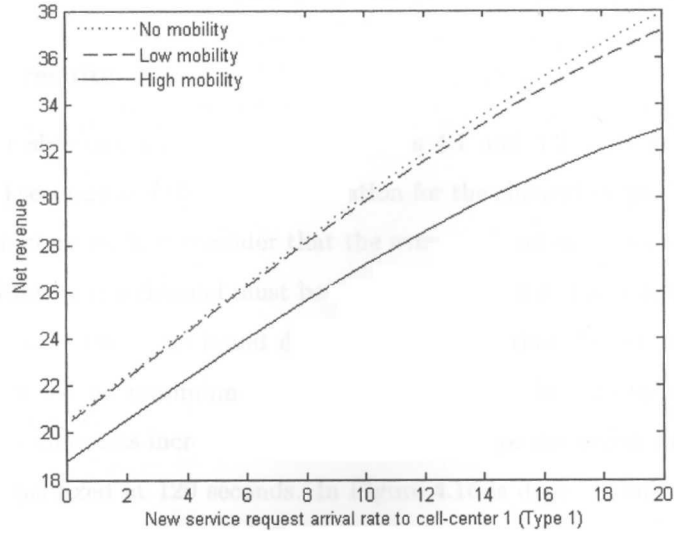


Figure 4.13: Comparison of the net revenue generated with different levels of mobility.

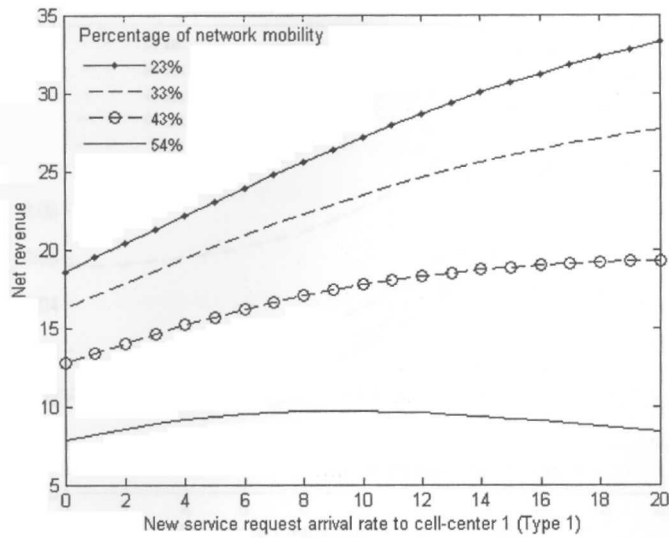


Figure 4.14: Net revenue with different levels of mobility.

4.2 Model for channel-aware conditions resource allocation.

In this section is presented the simulation results, where the wireless channel is time variant as was said earlier, so the number of resources blocks to be allocated not only depends on their availability but also if they are under reliable or unreliable conditions channel when a new service request has been requested. In chapter three was derived equations which reflects the impact of

the time-varying channel on the blocking probability of the resources blocks.

4.2.1 Blocking results

Parameters for simulation are taken from Tables 4.1 and 4.2, only is add the average bad state duration of 60 seconds and the average duration for the channel in good state of 120 seconds. To select this parameters we first consider that the average duration of a call is 120 seconds so in this time the condition of the channel must be good and we add a time when the channel changes to bad conditions. Last time was found doing a simulation that deliver us a network blocking probability less than 2% as minimum in the case of low mobility, so we use as initial value 5 seconds and then the time was increased until 60 seconds where the target was meet, and the time for the good state was fixed at 120 seconds. In Figure 4.15 is depicted this simulation where the family of curves shows that as increases the average time the channel remains in the bad state (unreliable) the blocking probability decreases.

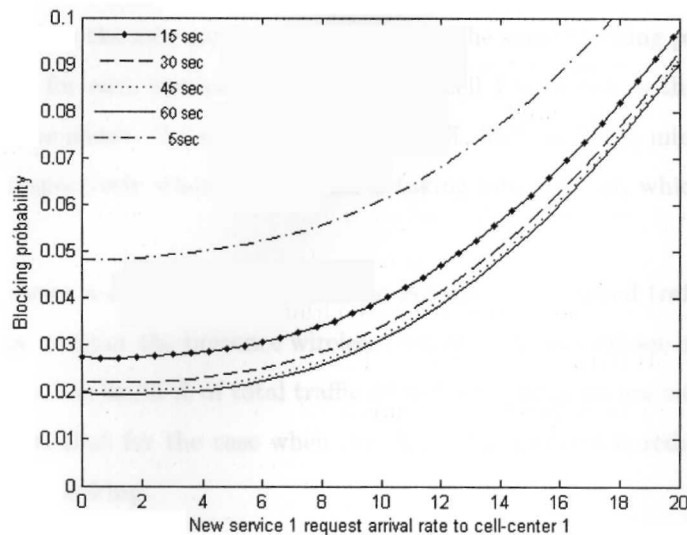


Figure 4.15: Bloking probability when a subcarrier go from a bad state to good state with different rates.

Figures 4.16 and 4.17 show the blocking probability in terms of the new request arrival rate, where it is seen that capacity is reduced when the channel is considered, because if a resource is in bad conditions then it appears to a user as not available, otherwise if that block were allocated the session requested may fail. In the last case the user would be more concerned that if we dot not assign him resources.

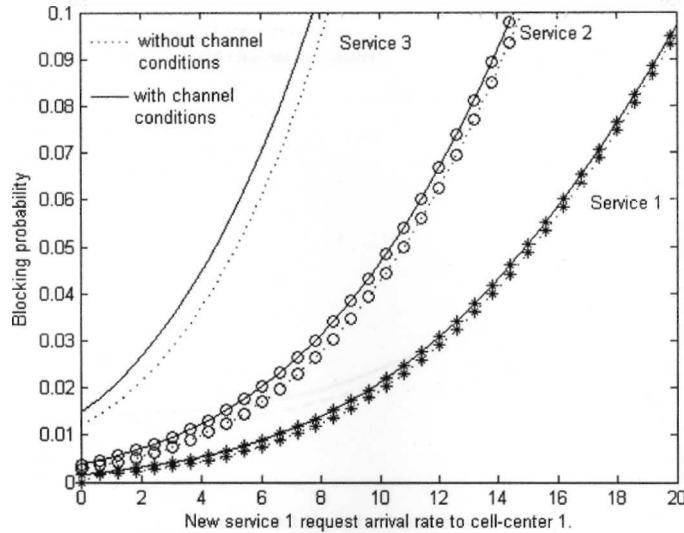


Figure 4.16: Blocking probability for all services at cell-center 1.

Figure 4.16 shows that although there is no mobility in the network, the availability of capacity has decreased, therefore the new service request rate for the same blocking probability is less. The blocking probability for each service at center area of cell 1 is shown, with and without channel conditions. As can be shown there is an increase of 34%, 35% and 33% minimum of blocking for service 1,2 and 3 respectively when the channel is taking into account, which reduces the carried traffic.

Figure 4.17, shows a comparison between the percentage of offered traffic to the network for no mobility, with or without the presence wireless channel. The percentage of the offered traffic to cell-center for service 1 is 28.83 % of total traffic offered when only we are calculating the blocking of the capacity, while that for the case when the channel has effects is reduced to 24.76%, to be under an acceptable blocking.

Figure 4.18 provides the blocking results when the user's session dwell time has ended, then him leaves the network and when the user go other area or cell. It can be shown that for the same total offered traffic to the network the offered traffic to cell 1 for service 1 has decreased with the following percentages 3.42%, 11.87% and 8.21% for no mobility, low and high mobility respectively. So with the same resources, less capacity can be allocated because of unreliable channel conditions and the users with high mobility as was seen in Figure4.10 are the most affected again.

This results reveals that influence of the channel when there is mobility made that blocking increases beyond of the permissible grade of service (2%) in a mobile wireless network.

Another scenario is presented when only a subcarrier must be under bad channel conditions to

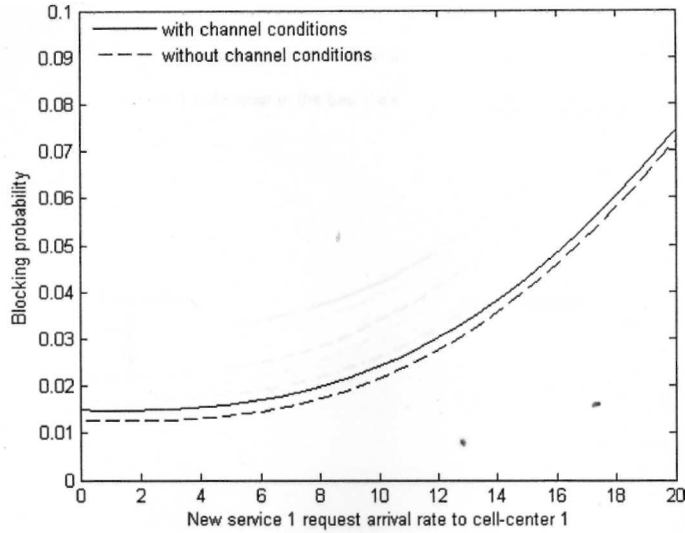


Figure 4.17: Comparison of network blocking for no mobility, under reliable and unreliable channel.

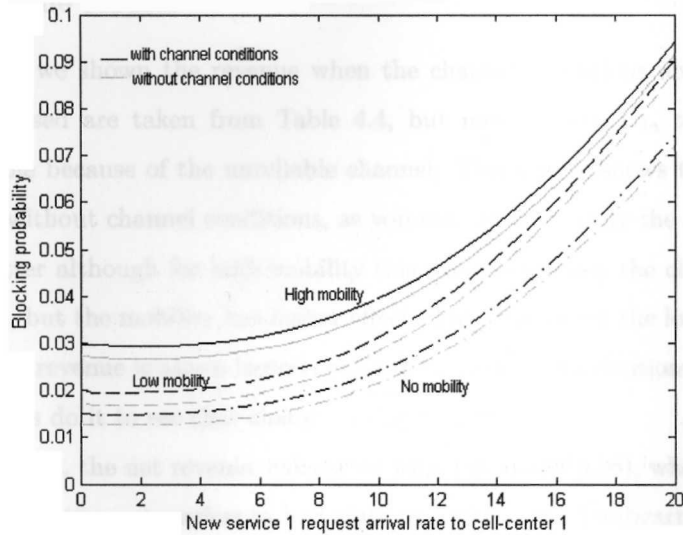


Figure 4.18: Comparison of blocking for the network with and without mobility.

consider that a resource block is not available. Figure 4.19 shows the network blocking probability calculated with Equation (3.24), where the mobility has different levels. In this scenario since it is only necessary that a subcarrier is in the bad state, the resource will be unavailable with higher probability, so the network blocking is higher than the scenario of a RB with 2 subcarriers in bad conditions. Latter condition showed, reveals that the resource blocks available will be less, then less users can be served.

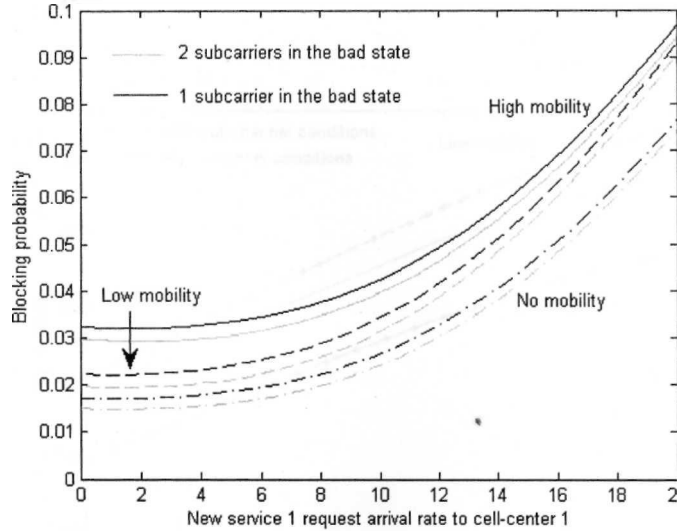


Figure 4.19: Network blocking when a resource block has 1 and 2 subcarriers under bad channel conditions.

4.2.2 Net revenue results

In Figure 4.20 we shown the revenue when the channel conditions are included, again the parameters to be used are taken from Table 4.4, but now the cost z_{la} take into account the channels unavailable because of the unreliable channel. This Figure shows the comparison of the revenue with and without channel conditions, as you can see when only the capacity is taken into account this is better although for high mobility this decreases, when the channel is included the revenue is reduced, but the mobility has higher effect. This can see for the low mobility, where the difference in the net revenue is almos imperceptible because the contribution of the channel is low, however a zoom in is do it to see that change in Figure 4.21.

Figure 4.22 shows, the net revenue calculated with Equation (3.26), where is compared when the resource block has two subcarriers in bad state and when only 1 subcarriers is affected by the channel. It is shown that the net revenue is fewer when the second scenario arises, because now the system has less capacity to be allocated so the less traffic is carried successfully.

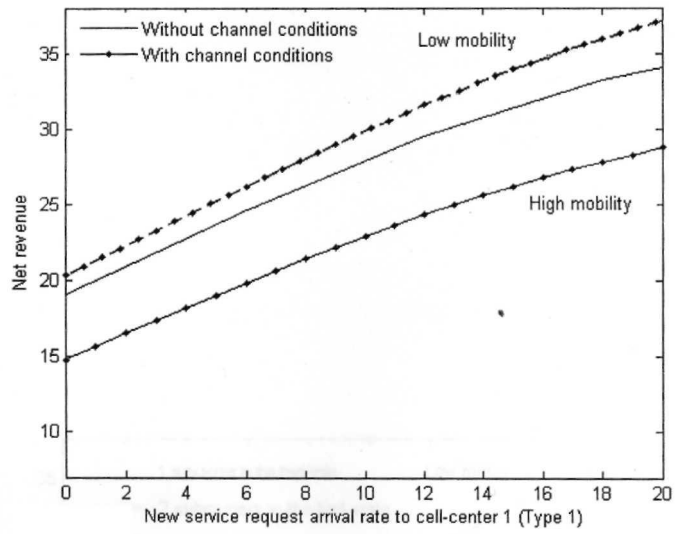


Figure 4.20: Comparison of the net revenue generated with a reliable and unreliable channel.

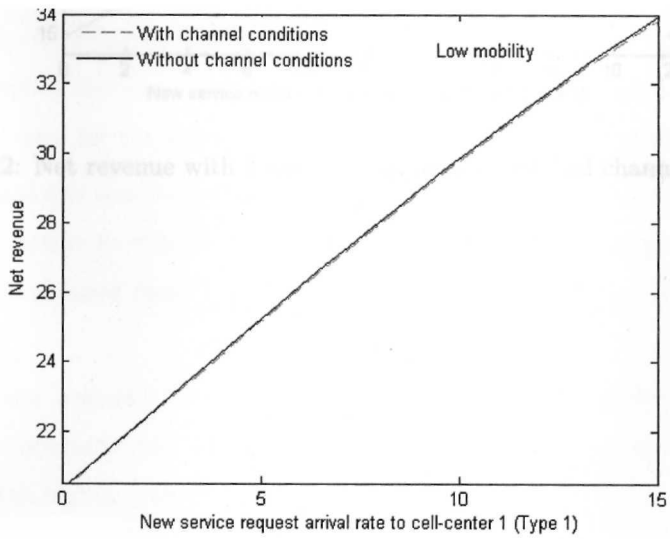


Figure 4.21: Net revenue with low mobility with and without channel conditions.

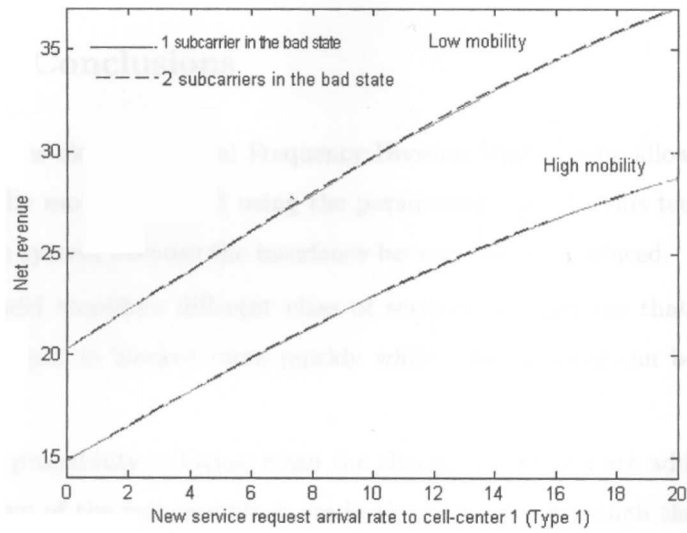


Figure 4.22: Net revenue with 1 and 2 subcarriers under bad channel conditions.

Chapter 5

Conclusions

This chapter contains the general conclusions of this work, as well as some future work to be developed are suggested.

5.1 General Conclusions

Using techniques like Orthogonal Frequency Division Multiplexing allowed me use the bandwidth efficiently, the model obtained using the parameters given by this technique improves the performance of the system because the interference between users is reduced.

Since the model considers different class of services, I could see that service with higher bandwidth requirement is blocked more quickly while other services can be requested by more users.

The blocking probability is higher when the channel conditions are added, i.e., when two of the three subcarriers of the resource block are in the bad state, although the new request arrival rate is the same as used for the scenario when the channel is not considered.

When I changed the condition that one subcarrier instead of two subcarriers of the RB is in the bad condition in order to consider that RB is not available, the blocking probability was higher, since the capacity is reduced faster because the available channels change to the unavailable state more quickly.

The net revenue revealed that a wireless system works better under low mobility because otherwise a service operator may be offer more traffic but the revenue will be less and the users will be blocking with higher probability.

The optimization on the net revenue gives useful information for a carrier that takes decisions according its capacity and the mobility of the users.

Finally with the model derived, the allocation can be done with lower computational complexity.

5.2 Future work

The model derived can be applied under other conditions, for example the reservation of channels for hand offs can be implemented. Other situation is when the number of subcarriers that contains a resource block can change dynamically, moreover the way to allocate them can be done in other way, for example depending on the signal to noise rate that each subcarrier has. Other parameter to be considered is the Average Fade Duration, since it reveals the behavior of the channel.

Bibliography

- [1] D. Bertsekas and R. Gallager, *Data Networks*. U.S.A.: Prentice Hall, Inc, 1992.
- [2] C. Vargas, M. V. Hedge, and M. Naraghi-Pour, "Implied costs in wireless networks," in *48th IEEE Vehicular Technology Conference*, pp. 904–908, 1998.
- [3] M. A. Aboelaze, "A call admission protocol for cellular networks that supports differentiated fairness," in *IEEE 59th Vehicular Technology Conference, 2004. VTC 2004-Spring*.
- [4] H. Rasouli and A. Anpalagan, "An asymptotically fair subcarrier allocation algorithm in ofdm systems," in *IEEE 69th Vehicular Technology Conference, 2009. VTC Spring 2009*.
- [5] S. Pietrzyk and G. J. Janssen, "Multiuser subcarrier allocation for qos provision in the ofdma systems," in *IEEE 56th Vehicular Technology Conference, 2002. Proceedings. VTC 2002-Fall*.
- [6] F. R. Farrokhi, M. Olfat, M. Alasti, and K. J. R. Liu, "Scheduling algorithms for quality of service aware ofdma wireless systems," in *IEEE Global Telecommunications Conference, 2004. GLOBECOM '04*.
- [7] J. Jang and K. B. Lee, "Transmit power adaptation for multiuser ofdm systems," *IEEE Journal on Selected Areas in Communications*, vol. 21, no. 2, pp. 171–178, February 2003.
- [8] G. Zhang, "Subcarrier and bit allocation for real-time services in multiuser ofdm systems," in *IEEE International Conference on Communications, 2004*.
- [9] S. Pietrzyk, *OFDMA for broadband wireless access*. USA: Artech House, Inc, 2006.
- [10] E. Dahlman, S. Parkvall, J. Skold, and P. Beming, *3G Evolution: HSPA and LTE for Mobile Broadband*,. Oxford: Elsevier, 2007.
- [11] A. F. Molisch, *Wireless Communications*. England: John Wiley & Sons,LTD, 2005.
- [12] S. Hara and R. Prasad, *Multicarrier Techniques for 4G Mobile Communications*. Artech House, 2003.
- [13] D. K. Sajal, *Mobile Handset Design*. John Wiley & Sons,LTD, 2010.

- [14] H. Schulze and C. Luders, *Theory and applications of OFDM and CDMA*. England: John Wiley & Sons, LTD, 2005.
- [15] K. Fazel and S. Kaiser, *Multi-Carrier and Spread Spectrum Systems*. England: John Wiley & Sons, LTD, 2003.
- [16] T. James, *Digital Techniques for Wideband Receivers*. Scitech, 2004.
- [17] G. Yuan, X. Zhang, W. Wang, and Y. Yang, "Carrier aggregation for lte-advanced mobile communication systems," *Communications Magazine, IEEE*, vol. 48, no. 2, pp. 88–93, 2010.
- [18] A. Furuskar, T. Jansson, and M. Lundevall, "The lte radio interface - key characteristics and performance," in *IEEE 19th International Symposium on Personal, Indoor and Mobile Radio Communications, PIMCR 2008*, pp. 1–5, 2008.
- [19] J. Berkmann, C. Carbonelli, F. Dietrich, C. Drewes, and W. Xu, "On 3g lte terminal implementation - standard, algorithms, complexities and challenges," in *International Wireless Communications and Mobile Computing Conference, 2008*.
- [20] H. Holma and A. Toskala, *LTE for UMTS - OFDMA and SC-FDMA Based Radio Access*. United Kingdom: John Wiley & Sons,LTD, 2009.
- [21] M. Rumney, "3gpp lte: Introducing single-carrier fdma," tech. rep., Agilent Measurement Journal, USA, January 2008.
- [22] G. Berardinelli, L. A. M. R. de Temino, S. Frattasi, M. I. Rahman, and P. Mogensen, "Ofdma vs. sc-fdma: Performance comparison in local area imt-a scenarios," *IEEE Wireless Communications*, vol. 15, no. 5, pp. 64–72, October 2008.
- [23] A. Technologies, "Agilent 3gpp long term evolution: System overview, product development and test challenges," tech. rep., Agilent Technologies, U.S.A., 2009.
- [24] L. A. M. R. de Temino, G. Berardinelli, S. Frattasi, and P. Mogensen, "Channel-aware scheduling algorithms for sc-fdma in lte uplink," in *IEEE 19th International Symposium on Personal, Indoor and Mobile Radio Communications*, pp. 1–6, 2008.
- [25] F. D. Clabrese, P. H. Michaelsen, C. Rosa, M. Anas, C. U. Castellanos, D. L. Villa, K. I. Pedersen, and P. E. Mogensen, "Search - tree based uplink channel aware packet scheduling for utran lte," in *IEEE Vehicular Technology Conference, 2008. VTC Spring 2008.*, pp. 1949–1953, 2008.
- [26] B. Bing, *Wireless Local Area, Networks*. John Wiley & Sons,LTD, 2002.

- [27] M. S. Gast, *802.11 Wireless Networks The Definitive Guide*. O'Reilly, 2002.
- [28] Y. Zhang, H. Hu, and M. Fujise, *Resource, Mobility, and Security Management in Wireless Networks and Mobile Communications*. New York: Auerbach, 2007.
- [29] S. Tomazic and G. Jakus, "Long term evolution: Towards 4th generation of mobile telephony and beyond," in *9th International Conference on Telecommunication in Modern Satellite, Cable, and Broadcasting Services, 2009. TELSIKS '09*.

Tecnológico de Monterrey, Campus Monterrey



30002007422439

<http://biblioteca.mty.itesm.mx>